DEPARTMENT OF CHEMISTRY, UNIVERSITY OF JYVÄSKYLÄ
RESEARCH REPORT No. 203

DESIGN AND CONSTRUCTION OF HALOGEN-BONDED CAPSULES AND CAGES

BY

LOTTA TURUNEN

Academic Dissertation for the Degree of
Doctor of Philosophy

To be presented, by permission of the Faculty of Mathematics and Science of the University of Jyväskylä, for public examination in Auditorium Kem4, on September 29th, 2017 at 12 noon.

UNIVERSITY OF JYVÄSKYLÄ

Jyväskylä, Finland
ISBN 978-951-39-7169-4 (print)
ISBN 978-951-39-7170-0 (electronic)
ISSN 0357-346X

ABSTRACT

Turunen, Lotta
Design and construction of halogen-bonded capsules and cages
Jyväskylä: University of Jyväskylä, 2017, 61 p.
(Department of Chemistry, University of Jyväskylä Research Report Series
ISSN: 0357-346X)
ISBN: 978-951-39-7169-4 (print), 978-951-39-7170-0 (electronic)

This thesis describes the design, synthesis and characterization of supramolecular halogen-bonded capsules and cages from multivalent ligands. In the first part of the thesis, an overview to halogen bonding is provided. After discussing the general features of the halogen bonding, the most frequently used halogen bond donors are introduced and examples of their utilization in halogen-bonded systems are discussed. The chapter also presents recent advances made in the field of halogen-bonded supramolecular capsules. The first part of the thesis also includes a review of halogen-bonded complexes involving halonium ions, and a brief introduction to [N···X$^+$···N] halogen bonds is provided along with a few examples of other three-center four-electron complexes.

The second part of the thesis outlines the design, synthesis and characterization of halogen-bonded assemblies, capsules and cages based on tetravalent resorcinarene cavitands and tripodal *N*-donor ligands. The results obtained are described in detail in the five publications.

Both halogen bond donors and acceptors were studied. Halogen bond donors functionalized with four haloacetylene moieties were used as tetravalent donors and their halogen bonding ability towards neutral and anionic halogen bond acceptors were studied in the solid state by single-crystal X-ray crystallography.

[N···I$^+$···N] halogen bonds were utilized in the formation of capsular assemblies from pyridine-functionalized cavitands. Based on the ligand design, dimeric and hexameric capsules were prepared through their structurally analogous metal-ligand coordination complexes. The formed complexes were characterized in solution and in the gas phase. [N···I$^+$···N] halogen bonds were further applied to the construction of halonium cages from tripodal *N*-donor ligands. For the first time, crystal structures of supramolecular cages constructed via multiple [N···I$^+$···N] halogen bonds were obtained.

Keywords: halogen bond, halonium ions, supramolecular chemistry, self-assembly, halogen-bonded capsules, cavitands, X-ray crystallography, cation exchange

Author's address

Lotta Turunen
Department of Chemistry
Nanoscience Center
P.O. Box 35
FI-40014 University of Jyväskylä
Finland
lotta.k.turunen@jyu.fi

Supervisors

Academy Professor Kari Rissanen
Department of Chemistry
Nanoscience Center
University of Jyväskylä

Adjunct Professor Ngong Kodiah Beyeh
Department of Applied Physics
School of Science, Aalto University

Reviewers

Professor Marc Fourmigué
CNRS Director of Research
"Matière Condensée et Systèmes Electroactifs" (MaCSE)
Institut des Sciences Chimiques de Rennes (ISCR)
RENNES, France

Professor Giuseppe Resnati
Department of Chemistry, Materials, Chemical Engineering "Giulio Natta"
Politecnico di Milano
Milan, Italy

Opponent

Professor Christer Aakeröy
Department of Chemistry
Kansas State University
Manhattan, Kansas, United States

ACKNOWLEDGEMENTS

This work was carried out at the Department of Chemistry, University of Jyväskylä, Finland during years 2013-2017. These years might have been the most demanding, frustrating and stressful of my life, but at the same time, these years have been the most rewarding, exciting and unforgettable. During this journey I have met a lot of great people, who I want to express my sincere gratitude.

First and foremost, I want to express my deepest gratitude to my supervisor, Academy Professor Kari Rissanen, for the opportunity to work in his group and introducing me in to the exciting world of supramolecular chemistry. I am grateful for all the advice, support and endless research ideas without forgetting the Savonian humor. I am also grateful for Adjunct Professor Ngong Kodiah Beyeh, my friend and supervisor, for all the guidance and encouragement throughout these years.

Professor Guiseppe Resnati and Professor Marc Fourmigué are greatly acknowledged for the detailed examination of this thesis. I am honoured to receive such supportive comments on my thesis from the leading scientists in the field of halogen bonding. I also thank Matti Nurmia for the language revision.

Professor Christoph A. Schalley and M. Sc. Ulrike Warzok are warmly thanked for the collaboration on mass spectrometric studies during and after my two research visits in Berlin. Adj. Prof. Manu Lahtinen and Dr. Anssi Peuronen are also thanked for another great collaboration.

Dr. Fangfang Pan, Dr. Rakesh Puttreddy and Dr. Arto Valkonen are greatly acknowledged for the endless patience and enthusiasm for going through all my crystallization samples and solving the crystal structures, whenever possible.

I would also like to thank all the staff and co-workers at the Department of Chemistry for creating such a great working environment. It has been a pleasure to work with all of you. Moreover, working here in Jyväskylä would not have been the same without the members of Rissanen group. Thanks for the friendship, support and discussions (scientific and non-scientific) during these years!

Special thanks go to the amazing group of people, who I have shared great moments both working and not working: Pia, Ondřej, Leticia, Toni, Filip, Sandra, Anniina, Hana and Jens. It has been the greatest journey with you! I would also like to say thank you to my dear friends Laura J., Susanna, Laura H., Jenni and Anu for taking my mind off work every now and then. Also, I want to thank the symphony orchestra of the University of Jyväskylä, Sinfis, for the music and members of Jyväskylä Floorbears for the great games.

Finally, I would like to thank my family for their endless support and always believing in me: mom and dad, Matias, Riikka, Neela, Aaro, Sami and Wilma. This would have not been possible without you! I also want to thank my grandparents for all the support and my cousin Sara for all the great adventures we have had together all the way from Jyväskylä to abroad and back!

Jyväskylä 1.9.2017

Lotta Turunen

LIST OF ORIGINAL PUBLICATIONS

This thesis is based on the following original publications which in the text are referred to by their Roman numerals.

I. L. Turunen, N. K. Beyeh, F. Pan, A. Valkonen and K. Rissanen, Tetraiodoethynyl resorcinarene cavitands as multivalent halogen bond donors, *Chem. Commun.* **2014**, *50*, 15920 - 15923.

II. L. Turunen, U. Warzok, R. Puttreddy, N. K. Beyeh, C. A. Schalley and K. Rissanen, [N···I$^+$···N] Halogen-Bonded Dimeric Capsules from Tetrakis(3-pyridyl)ethylene Cavitands, *Angew. Chem. Int. Ed.* **2016**, *55*, 14033–14036.

III. L. Turunen, U. Warzok, C. A. Schalley and K. Rissanen, Nano-sized $I_{12}L_6$ Molecular Capsules based on the [N···I$^+$···N] Halogen Bond, *Chem.* **2017**, *in press.* DOI: 10.1016/j.chempr.2017.08.010

IV. L. Turunen, A. Peuronen, S. Forsblom, E. Kalenius, M. Lahtinen and K. Rissanen, Tetrameric and Dimeric [N···I$^+$···N] Halogen-Bonded Supramolecular Cages, *Chem. Eur.J.* **2017**, *23*, 11714 –11718.

V. L. Turunen, F. Pan, N. K. Beyeh, M. Cetina, J. F. Trant, R. H. A. Ras and K. Rissanen, Halogen-bonded Solvates of Tetraethynyl Cavitands, *CrystEngComm*, **2017**, *in press*, DOI: 10.1039/C7CE01118K

Author's contribution

The author carried out all the synthetic work excluding the ligand **60** in paper **IV**. She carried out most of the characterizations, NMR experiments and crystallization trials and was involved in mass spectrometric measurements in papers **II-III**. The author has been actively involved in the writing process of all five publications and has written the first drafts of the papers **I-IV**.

CONTENTS

ABBREVIATIONS

ACN	acetonitrile
Bu_3S^+	tributylsulfonium
D	diffusion coefficient
DABCO	1,4-diazabicyclo[2.2.2]octane
DCM	dichloromethane
DIPFA	α,ω-diiodoperfluoroalkane
DMF	dimethylformamide
DOSY	diffusion-ordered spectroscopy
ESI-MS	electrospray ionization mass spectrometry
Et_3BuN^+	triethylbutylammonium
Et_4N^+	tetraethylammonium
Et_4P^+	tetraethylphosphonium
HB	hydrogen bonding
HMBC	heteronuclear multiple bond correlation
HMTA	hexamethylenetetramine
IR	infrared
L	ligand
M	metal
Me	methyl
Me_3S^+	trimethylsulfonium
NBS	*N*-bromosuccinimide
NIS	*N*-iodosuccinimide
NISac	*N*-iodosaccharin
NMR	nuclear magnetic resonance spectroscopy
OTs	*p*-toluenesulfonate
PFHC	perfluorohalocarbon
PPh_3	triphenylphosphine
PPN^+	bis(triphenylphosphine)iminium
Pr_4N^+	tetrapropylammonium
Py	pyridine
^{t}Bu	*tert*-butyl
THF	tetrahydrofuran
TPA	tetrapropylammonium
XB	Halogen bond
3*c*4*e*	three-center four-electron

1 INTRODUCTION

1.1 Halogen bonding

Halogen atoms in organic compounds are generally considered negative in their character due to their high electronegativity. However, in compounds where a halogen atom forms covalent bond(s), the electron density is anisotropically distributed and an area of lower electron density is created along the extension of the covalent bond.[1] If the electron deficiency is sufficient, this can lead to the formation of a region where the electrostatic potential is positive. This region (called a σ-hole) can now interact with negative sites of molecules. This somewhat counterintuitive way of halogen atoms to interact with nucleophilic species is nowadays called halogen bonding (XB).

The tendency of halogens to interact with atoms containing lone electron pairs was recognized already in the 19th century, when the ability of I_2 to interact with NH_3 was discovered.[2] Nevertheless, it took another century before the pioneering work on charge-transfer interactions by R. S. Mulliken[3] (Nobel Prize in chemistry in 1966) and O. Hassel[4] (Nobel Prize in chemistry in 1969) gave some insight in to the nature of such donor-acceptor complexes. Particularly, the extensive X-ray crystallographic studies by Hassel provided valuable information of the interaction between dihalogens or halocarbons with electron donor molecules.[5–9] In 1954 one of the first solid state cases of halogen bonding was revealed, when X-ray quality crystals were obtained from a 1:1 mixture of bromine and 1,4-dioxane (figure 1).[5] The crystal structure found was an infinite linear chain of alternate bromine and 1,4-dioxane molecules, where the Br⋯O distances were shorter than the sum of their respective van der Waals radii and the bond angle of Br−Br⋯O was close to 180°.

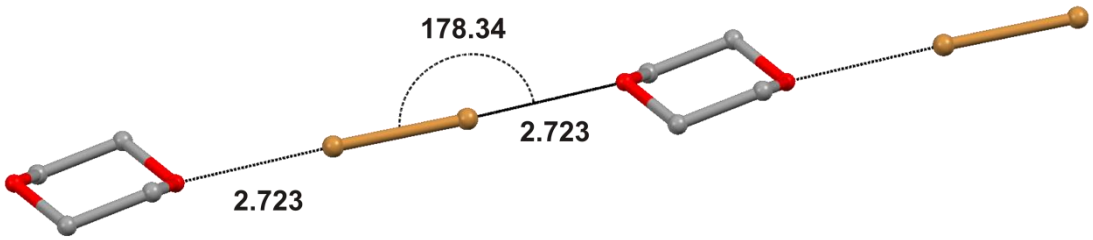

FIGURE 1 Crystal structure of the polymeric 1:1 XB complex of 1,4-dioxane and bromine (CSD ref. code: DOXABR).[5]

In the following years, more research on such intermolecular interactions involving halogen atoms was conducted.[10,11] The real turning point for halogen bonding was during the millennium, when A. Legon started a systematic analysis of geometries and charge distributions of various types of halogen-bonded adducts formed in the gas phase.[12,13] At about the same time Resnati, Metrangolo and co-workers took a closer look at the interactions of perfluorinated haloalkanes and –benzenes with atoms possessing lone pairs.[14–16] Their pioneering work highlighted the impact of halogen bonding as a recognition motif in self-assembly processes and started the "rediscovery" of halogen bonding.

From the beginning of the 21st century, more researchers started to notice the potential of halogen bonding as a new recognition motif. Since XB can form predictable and highly directional interactions in the solid state, in solution and in the gas phase, it has found place in a wide variety of contemporary chemical research fields including crystal engineering, material science and medicinal chemistry.

The term "halogen bond" was probably first introduced by Zingaro and Hedges in 1961 to describe complexes formed in solution by halogens or interhalogens with phosphine oxides and sulfides.[17] Then the term began to be used for other related systems.[18–20] Nevertheless, it took more than five decades before the actual definition for halogen bonding was given in 2013. In the recommendation of the International Union of Pure and Applied Chemistry (IUPAC) states "*A halogen bond occurs when there is evidence of a net attractive interaction between an electrophilic region associated with a halogen atom in a molecular entity and a nucleophilic region in another, or the same, molecular entity.*"[21] According to this definition, a halogen bond can generally be denoted as R-X···Y, where R-X is the XB donor and Y is the XB acceptor. X is any covalently-bonded halogen atom with an electrophilic region. Halonium ions (X^+) can also behave as XB donors and form three-center four-electron XBs. In an R-X···Y system, the X···Y distance is shorter than the sum of the van der Waals radii of the interacting atoms and a concomitant lengthening of the covalent R-X bond is typically observed. The bond angles in R-X-Y are generally close to 180°.

1.1.1 Nature of halogen bonding

While halogen bonding has become a widely applied interaction in a variety of chemistry fields, understanding of the origin and characteristics of this interaction has become more important. Over the last decade, the chemical nature of the halogen bond has been the focus of many theoretical studies. However, an analysis that could satisfactorily explain all the characteristics of XB has not yet been achieved, and therefore, the chemical nature of this bond is still a matter of debate.

The nature of the halogen bond was first rationalized by the σ-hole concept introduced by Politzer and co-workers.[22] Computational studies on CF_3X molecules (X = F, Cl, Br, I) revealed the formation of a region of positive electrostatic potential (the σ-hole) on the outermost portion of the halogen's (Cl, Br, I) surface due to the anisotropical distribution of electrons of covalently-bonded halogen atoms. The three unshared electron pairs produce a belt of negative electrostatic potential around the central part of X.[22] Halogen bonding could then be seen as an electrostatically driven interaction between the σ-hole of a covalently-bonded halogen atom X and a negative site of Y, resulting in the formation of a linear complex R-X···Y.[23] The σ-hole concept explained empirically observed features of halogen bonding: how halogen atoms can behave as electrophiles and why they form close to linear structures with nucleophiles (figure 2).

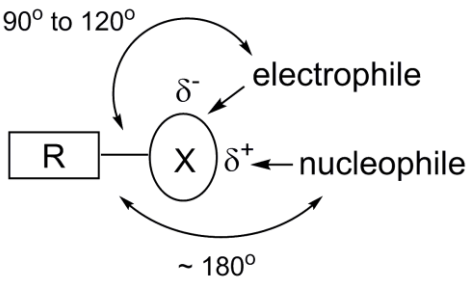

FIGURE 2 Schematic presentation of the anisotropic distribution of the electron density around covalently bound halogen atoms.[23]

Accordingly, the XB ability of a molecule would depend on the polarizability and electronegativity of the halogen atom and the electron withdrawing power of the R-group.[23] The strength of the halogen bond would depend on the positive character of the corresponding σ-hole; the XB donor ability of RX could thus be increased with a more electronegative R-group. However, an unexpected trend was discovered in the strengths of halogen-bonded adducts of CY_3I (Y = F, Cl, Br, I) with chloride and trimethylamine.[24] Computational studies showed that the donor strength of a compound R–X does not necessarily increase with higher electronegativity of the (carbon-based) R-group. This phenomenon could not be fully explained by the electrostatic effects of the σ-hole and therefore, the quantum chemical effects, *e.g.* charge-transfer

interactions and the Pauli repulsion, were suggested to have an impact.[24] Furthermore, the directionality of the XB was observed to result from increased charge-transfer stabilization and reduced lone-pair repulsion in linear adducts.[25] Along with electrostatic and quantum chemical effects, dispersion and polarization are also suggested to have an impact on XB interactions.[11,26]

Even though the exact nature of the XB is not yet fully understood, it has become gradually clearer that several effects can influence in the formation of halogen bonds and these bonding characteristics are highly dependent on the interacting species.

1.1.2 General features of halogen bonding

Due to similarities in the interactions, *e.g.* geometric and energetic parallels, halogen bonding R-X···Y is generally compared to hydrogen bonding (HB) R-H···Y. Both interactions are directional and hence, the geometries of the formed complexes can be well predicted. However, there are also significant differences between XB and HB. For example, XB is typically more hydrophobic than HB leading to different solvent dependencies.[27] Halogen atoms are also larger than hydrogen atoms, which makes XB donors more sensitive to steric effects.

All four halogens are able to form XBs, yet fluorine differs from others. The ability of the halogens to act as XB donors generally follows the order F << Cl < Br < I, which can be generally explained by the polarizability of the halogen atoms. In covalently-bonded halogen atoms the electrostatic potential remains mostly negative for F atoms, whereas Cl, Br and I atoms have also an area of positive charge (σ-hole).[22] The ability of fluorine to behave as an XB donor has been questioned, but there is theoretical and experimental evidence that under specific conditions fluorine can also form halogen bonds.[28,29]

The strength of the XB interactions varies roughly from 10 kJ/mol to 180 kJ/mol depending on the donor and acceptor used.[30] For example, Cl⋯ Cl interactions between chlorocarbons are among the weakest observed; the strongest known so far is the interaction between $I^- \cdots I_2$ in I_3^-.[30] The strength of the XB can be tuned by changing the halogen atom and electron withdrawing ability of the R-group covalently-bonded to the halogen atom. This means that a moiety that can enhance the anisotropy of the electron distribution of the X, is expected to form stronger XB donor molecules leading to strong XBs. Even though the correlation of the strength to the bond length is not fully accepted in terms of shorter bond distances meaning stronger XB interactions, it was observed that N···I distances were decreased in cocrystals of 4-(*N*,*N*-dimethylamino)pyridine with fluorinated iodobenzenes by increasing the number of fluorine atoms in the benzene core.[31] In halocarbons the donor strength of the covalently-bonded halogen atom increases in the order $C(sp^3) < C(sp^2) < C(sp)$ when there are no other structural differences present.[30]

XB is a highly directional interaction and it prefers linearity in the formed complexes. In R-X···Y systems, the bond angle between the covalent and non-

covalent bonds is generally close to 180° due to the localization of the σ-hole on the elongation of the R-X covalent bond.[22]

In XB complexes, the directionality of the interaction and the geometry of the formed adducts are not only controlled by the donor and the σ-hole, but also the acceptor plays a role. Generally, anions, molecules containing lone electron pairs or systems containing π-electrons can behave as XB acceptors and all acceptors have different geometric preferences. Acceptors involving heteroatoms Y with a lone electron pair generally form the XB along the axis of the donated electron pair on Y. If the acceptors are π electrons of an unsaturated system, the donor is perpendicular to the π system. Due to their spherical nature, halide anions are able to adapt a variety of coordination numbers and hence, several R-X···X$^-$···X-R angles have been observed.[32] Examples of geometric features of diiodoperfluorobenzene with different lone-pair acceptor moieties are presented in figure 3.

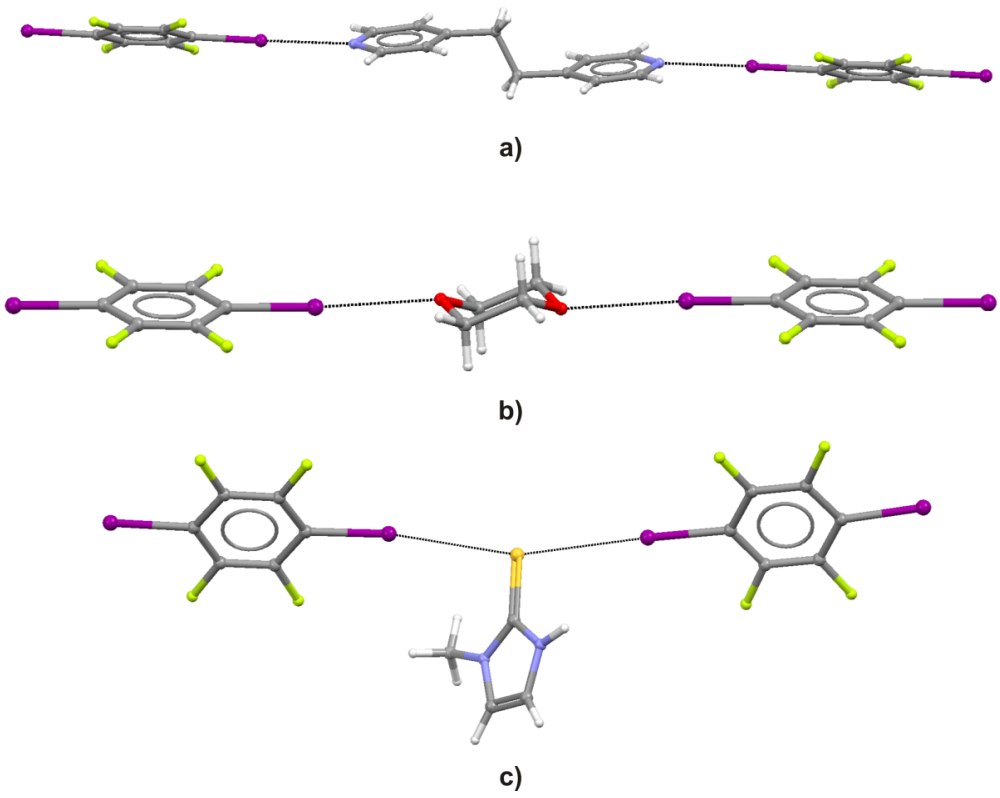

FIGURE 3 Crystal structures of XB complexes formed between 1,4-diiodotetrafluorobenzene and a) 1,2-bis(4-pyridyl)ethane, b) 1,4-dioxane and c) thiamazole showing the geometric features of XB (CSD ref. codes: DIVDAO, EDAGIZ, MEKWOO).[15,33,34]

The interaction ratio $R_{XB} = d_{XB}/(X_{vdw}+B_{vdw})$, where the distance d_{XB} between the donor (X) and acceptor (B) is divided by the sum of their van der Waals radii can be used to compare XB distances of different XB systems.[11,35,36] R_{XB} has also been used to give rough estimates of the strength of the

interactions in the solid state. However, as mentioned above, the interaction distance does not unambiguously correlate with the real strength of the XB.

1.1.3 XB donors

Since the first examples of halogen-bonded complexes, dihalogens and interhalogens have been widely applied in the formation of halogen-bonded adducts with halides and molecules containing lone pairs. As XB has become a more applied interaction, also the need for developing more sophisticated and tunable donor and acceptor systems has arisen.

The frequently used XB donors and their utilization in halogen-bonded systems are discussed in the following sections.

1.1.3.1 Perfluorohalocarbons

Among the group of XB donors, perfluorohalocarbons (PFHCs) are by far the most studied and applied. The PFHCs have advantages compared to the corresponding hydrocarbon analogues.[16] While fluorine atoms are strongly electronegative, the electron accepting ability of other halogen atoms (Cl, Br, I) in PFHCs is generally higher than that of the corresponding hydrocarbon analogues. In the seminal work of Resnati, Metrangolo and co-workers, PFHCs were used as ditopic XB donors and different halogen-bonded architectures were constructed with neutral, ditopic acceptors possessing lone pairs, typically nitrogen-containing compounds.[14,15,37,38] The use of ditopic donor and acceptor moieties was a simple, yet effective strategy for building halogen-bonded networks, and desired crystals were generally obtained from equimolar mixtures of XB donor and acceptor. Aliphatic and aromatic PFHCs have been subsequently applied in crystal engineering; halogen-bonded architectures based on neutral molecules connected through N···X[35–37], O···X[42] and S···X[34] interactions or through anionic acceptors[43] have been reported.

α,ω-Diiodoperfluoroalkanes (DIPFAs) are key intermediates in the synthesis of various fluorochemicals and –polymers, but their production in high yield and purity is difficult.[44] In 2009, it was discovered that DIPFAs could be selectively and reversibly encapsulated by means of halogen bonding.[44] By mixing bis(trimethylammonium) alkane diiodides and DIPFAs, cocrystals through $I^-\cdots I(CF_2)_mI\cdots I^-$ XBs were obtained (figure 4). The process was found to be highly selective, as the formation of the cocrystals was found to depend on the length of both components: the length of the formed $I^-\cdots I(CF_2)_mI\cdots I^-$ had to match the length of the bis(trimethylammonium) alkane cation (figure 4). Therefore, DIPFAs 2 to 12 carbons long could be isolated from mixtures by crystallizing them together with size-matching bis(trimethylammonium) alkane diiodides. Furthermore, a microcrystalline powder of the iodide salt was found to selectively capture the DIPFAs from the gas phase.

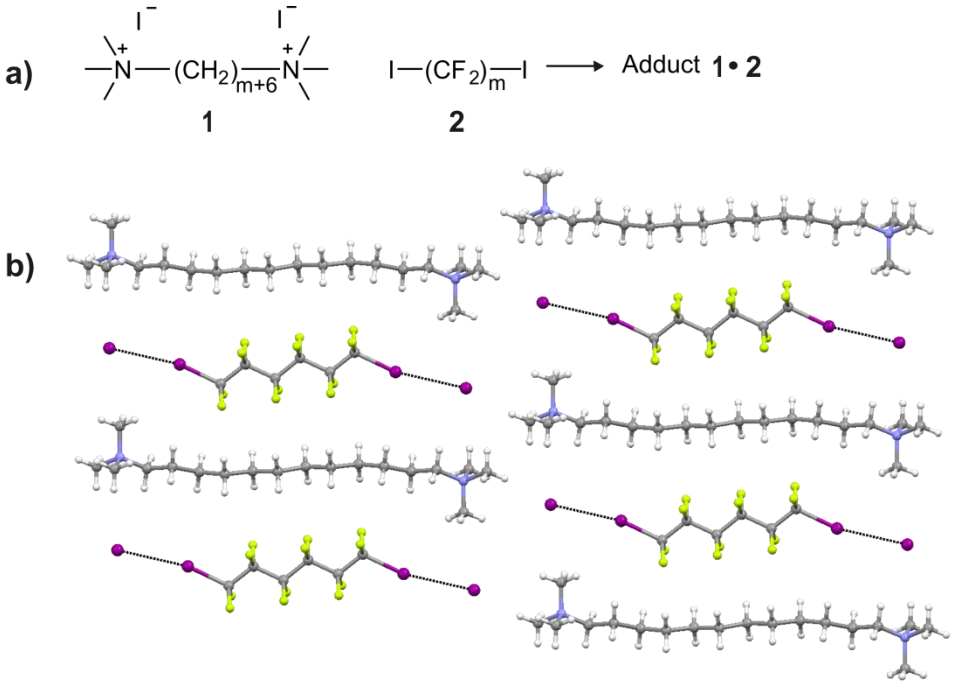

FIGURE 4 a) Schematic presentation of the formation of cocrystals (m = 2, 4, 6, 8, 10, 12) and b) crystal structure of bis(trimethylammonium) alkane diiodides encapsulating 1,6-diiodoperfluorohexane (CSD ref. code: XOVBOV).[44]

Perfluorohaloarenes have been utilized as XB donors as themselves or as structural parts of the donor molecules. In general, by changing the number and relative positions of the fluoro and, in most cases, iodo or bromo substituents at the benzene core, mono-, di-, tri- or multivalent donors can be achieved and a variety of halogen-bonded architectures can be obtained.[45–48] However, increasing the number of XB donor moieties in a single aromatic system does not always result in multivalent halogen bond systems, as observed by van der Boom and co-workers.[49] The 1,3,5-trifluoro-2,4,6-triiodobenzene **3** was expected to behave as a tridentate XB donor and form (6,3) networks with bipyridyl derivatives. However, the N···I interactions were observed to weaken with more nitrogens coordinated to **3**, resulting in formation of infinite chains where **3** behaved as divalent donor.

By changing the neutral bipyridyl derivative acceptors to stronger anionic ones, Metrangolo, Resnati and co-workers were able to crystallize **3** with iodide salts as desired honeycomb-like (6,3) networks (figure 5).[50] The formation of the networks was strongly influenced by the size of the counterions: the smallest counterions were able to stabilize the planar honeycomb networks, whereas more and more corrugated networks were obtained by increasing the cation size.

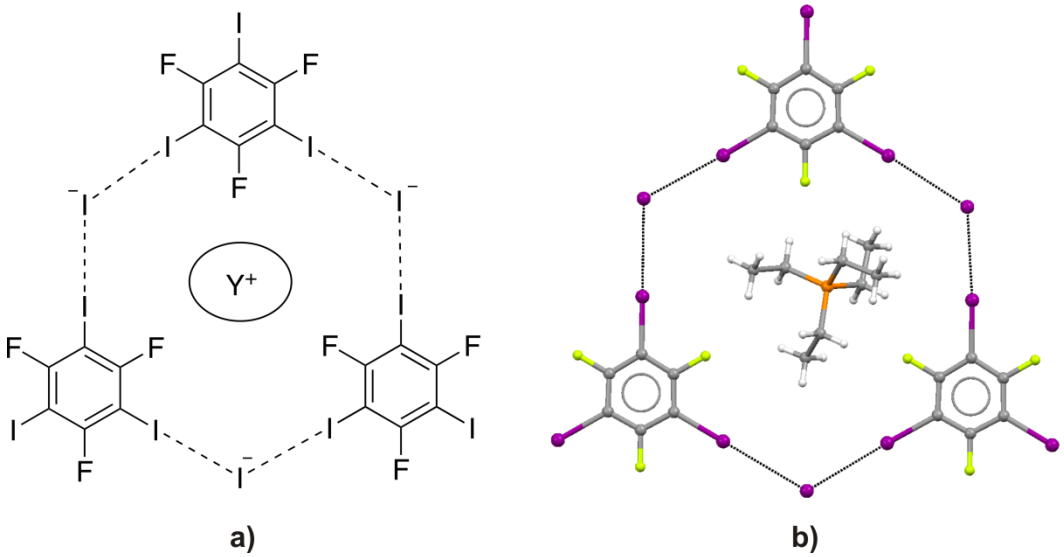

FIGURE 5 a) Schematic presentation of the (6,3) network formed between **3** and iodide salts (Y = Me_3S^+, Et_4N^+, Pr_4N^+, Et_4P^+) and b) crystal structure of tetraethylphosphonium iodide network (CSD ref. code: CIZSAG).[50]

Pentaerythritol tetrakis(4-iodo-2,3,5,6-tetrafluorophenyl) ether **4** is a tetradentate XB donor, which has been used in the construction of highly interpenetrated networks based on N···I interactions.[51] Crystallization of tetradentate donor and acceptor, **4** and tetrakis(4-pyridyl)pentaerythritol **5**, in a 1:1 ratio led to the formation of a remarkable tenfold diamondoid network. The same strategy to create 3D architectures was used earlier by Desiraju and coworkers: the self-assembly of 4,4′-diiodo-4′′,4′′′-dinitrotetraphenylmethane **6** resulted in a formation of diamondoid network based on I···O_2N interactions.[52] More detailed studies of the solid-state structure revealed the formation of an interpenetrated system constructed of 5-fold diamondoid and 3-fold square grid networks.

NMR spectroscopy has become the most powerful tool to study XBs in solution, as tiny electron density alterations can be detected. First research of XB in solution was done by mixing the PFHC donor molecules in the solvent, which behaved simultaneously as an XB acceptor.[53] More sophisticated systems were developed for anion sensing through halogen bonding (figure 6).[54,55] Multivalent *para*-substituted iodotetrafluorobenzene derivative **7** was utilized in anion sensing by exploiting NaI ion-pair recognition.[54] Solution studies revealed a modest but measurable affinity of the receptor towards sodium iodide. As the affinity was found to be 20-fold higher than the affinity of the analogous non-halogenated perfluoro-receptor, the stronger binding was expected to result from halogen bonding. Also, the crystal structure of the complex between the receptor **7** and NaI confirmed the C-I···I^- interaction. Competition experiments by tandem ESI-MS/MS revealed a higher affinity of I^- in the presence of Cl^- and Br^--anions.

Because the use of receptor **7** resulted in divergent arrays instead of orienting the donor in a more convergent way, as generally required for a high-

affinity host, Taylor and co-workers designed monodentate, bidentate and tridentate ligands based on *ortho*-substituted iodoperfluoroarenes for anion sensing solely by halogen bonding.[55–57] The designed hosts oriented the PFHC substituents appropriately for the formation of multiple XBs with halide anions. The highest binding affinity in acetone-d_6 was achieved with tripodal ligand **8** (figure 6), which was found to selectively bound Cl^-.

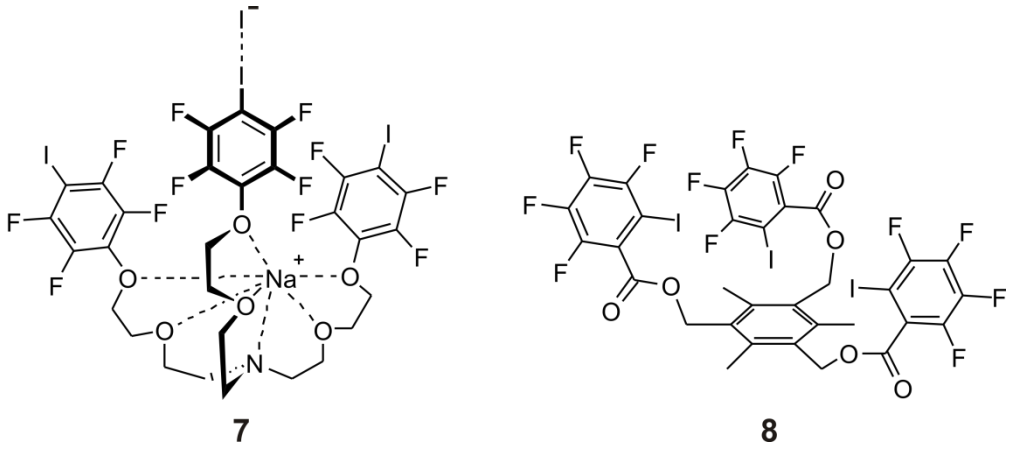

FIGURE 6 Structures of the anion receptors **7** and **8** based on PFHCs.[54,55]

The halogen bonding ability of PFHCs was also utilized by Huber and co-workers, who designed and synthesized ligands **9**, **10** and **11** (figure 7) and used them as neutral multidentate PFHC XB donors in organocatalysis.[58] The catalytic activity of ligands **9**, **10** and **11** was tested in a reaction of 1-chloroisochroman with ketene silyl acetals and the results supported the ability of XBs to catalyze reactions. A strong dependence on the number and the relative orientation of the iodine substituents was also found, because the ligands **9** and **11** were found to catalyze the reaction, while ligand **10** did not.[58]

Huber and coworkers continued their work with ligand **11** and with a topolocigally simpler ligand **12,** and studied their three-point XB formation in the solid state with triamine **13**.[59] As expected, in the X-ray structures of the complexes of **11** or **12** and **13**, each of the iodines of the ligands **11** and **12** are halogen-bonded to the nitrogens of **13** (figure 7). Three-point XBs were studied further in solution with ligand **12**. ^{19}F NMR titration experiments revealed that the binding of **12** to **13** was significantly higher than that of the comparable monodentate amine. Followed-up studies of multivalent PFHC based donors **9**, **10** and **11** revealed different binding behaviour of chloride, bromide and iodide anions in solution, in the solid state and in (calculated) gas phase.[60]

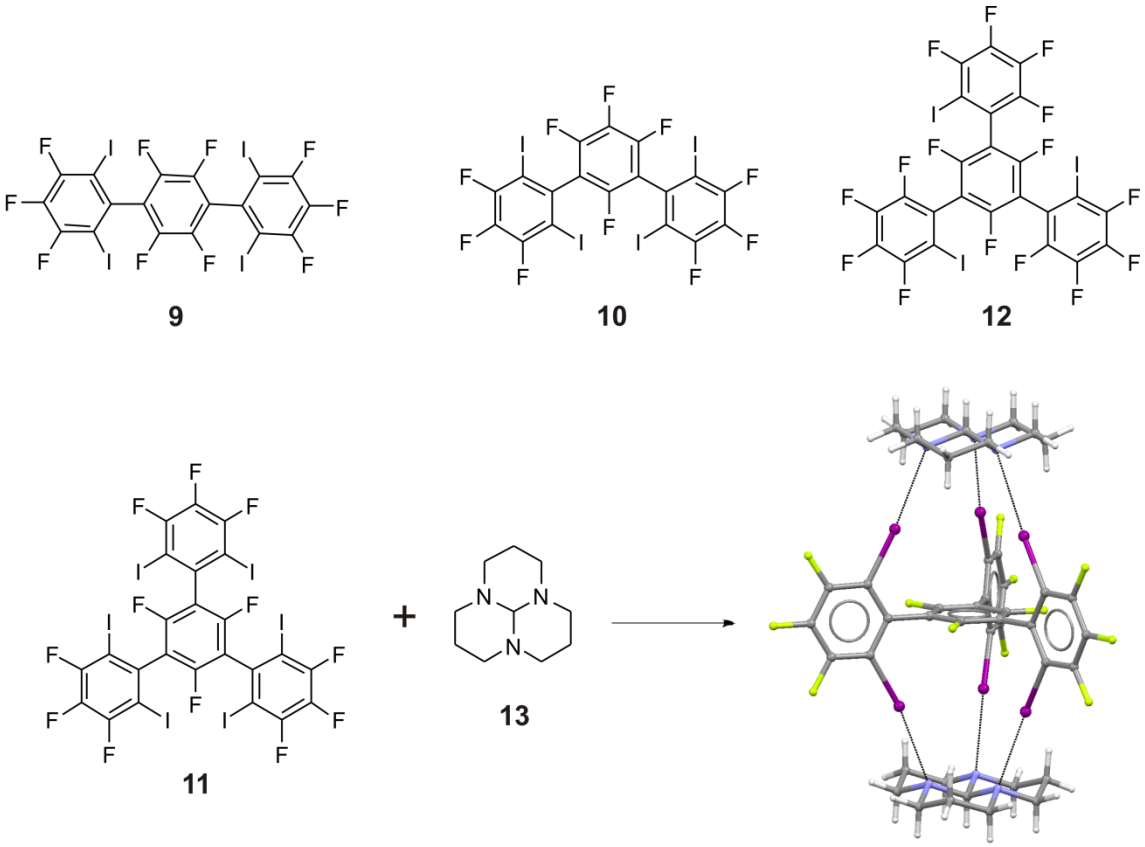

FIGURE 7 Structures of perfluoroarene ligands **9**, **10**, **11** and **12** and crystal structure of XB complex of **11** and **13** (CSD ref. code: LORQUG).[59]

PFHCs have also been utilized in material science to add new features, for example, to liquid crystals[61–63], polymers[64,65] and gels[66]. It was discovered by Bruce and co-workers that XB can be used to induce mesomorphism in non-mesomorphic components.[61] Liquid-crystalline complexes were prepared by exploiting N···I interaction between iodopentafluorobenzene and different nonmesomorphic 4-alkoxystilbazoles. The formation of the XB complexes was proven by colour change of the product and more directly by X-ray diffraction (figure 8a). In the extension of the work, acceptors were changed to ditopic aliphatic PFHCs; the formed trimeric complexes showed liquid-crystallinity (figure 8b).[62] PFHCs were also utilized by Xu and co-workers in designing high molecular weight supramolecular liquid crystals.[63]

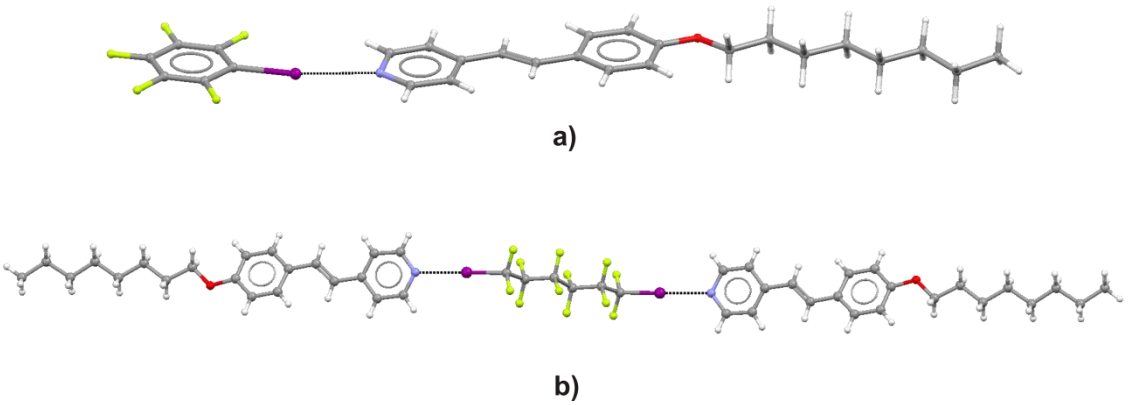

FIGURE 8 Crystal structures of halogen-bonded liquid crystals utilizing a) aromatic PFHCs (CSD ref. code: IQEWIK)[61] and b) aliphatic PFHCs (CSD ref. code: DENMIT).[62]

The formation of polymers controlled by XB interactions has been reported. XB interactions between poly(4-vinylpyridine) **14** and diiodoperfluoroalkanes resulted in the formation of comb-shaped polymers.[64] Aliphatic PFHCs have also been used to control and direct the self-assembly of polymers.[65]

Using PFHCs, either as structural parts in a gelator molecule or as a gel-forming partner, Steed and co-workers were able to form halogen-bonded supramolecular gels in polar organic solvent-water mixtures.[66] The crystal structure of a 1:1 complex of 1,4-diiodotetrafluorobenzene **15** and bis[(1-methyl-1-(3-pyridylureido)ethyl]benzene **16** confirmed that the gel formation was driven by XB interactions between iodine of the PFHCs and pyridyl nitrogen, which simultaneously hindered the competing gel-inhibiting pyridyl-urea interactions.

1.1.3.2 Haloacetylenes

Haloacetylenes are generally used in organic synthesis, but their role as XB donors has received less attention. The ability of haloacetylenes to interact with nucleophiles was discovered already in the early 20th century, when diiodoacetylenes were found to interact with nitrogen-containing bases.[67] Solid state evidence of such interactions was provided in 1960's, when the crystal structures of iodo-, bromo-, and chlorocyanoacetylenes were reported.[68,69]

Haloacetylenes can form halogen bonds with a variety of acceptors in the solid state[70–72] and in solution[73]. Furthermore, haloacetylenes were found to form as strong interactions as pentafluoroiodobenzenes, as evidenced by a combination of structural chemistry, IR spectroscopy and calculations.[74]

Diiodopolyynes I–(C≡C)$_n$–I are linear ditopic XB donors that have drawn attention mainly due to their potential to be precursors to conjugated polymers. Goroff and co-workers speculated that diiodopolyalkyne monomers could be correctly aligned for topochemical polymerization by forming XB adducts with Lewis bases.[75] The assumption was proven correct: the alignment of diiodobuta-1,3-diyne **17** with bis(nitrile)oxalamide **18** resulted in spontaneous

formation of poly(diiododiacetylene) **19** under crystallization conditions (figure 9).[76]

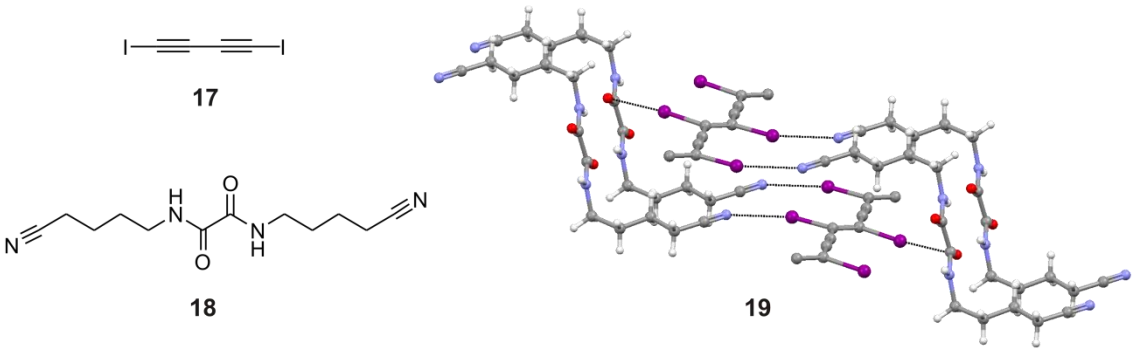

FIGURE 9 Structures of the **17** and **18** and the crystal structure of the spontaneously formed poly(diiododiacetylene) **19** (CSD ref. code: CEKFOO).[76]

Yamamoto and co-workers developed a series of halogen-bonded networks to create conducting nanowires based on organic radical cations.[77–81] In these structures, nanowires are formed when tetrathiafulvalene-based radical cations are arranged in layers by halogen-bonded networks consisting of ditopic acetylene- or tetratopic tetraiodoethylene XB donors and halide anions, the counter anions of radical cations.[77–79] During the preparation of more insulating materials, tetratopic XB donor **20** was developed (figure 10).[80] Iodoacetylenes of **20** form XBs either with chloride anions or with the ethynyl carbons of the neighbouring donor molecule (figure 10). In order to further develop insulating materials, pseudotetrahedral donor **21** was synthesized.[81] Increasing the size of the tetratopic donor led to the formation of PtS-type structures with 8-fold interpenetration. Each of the acetylenic iodines form XBs with chloride or bromide, and each halide anion behaves as a tetradentate XB acceptor towards four iodines of different donor molecules resulting in the formation of square planar motifs (figure 10).

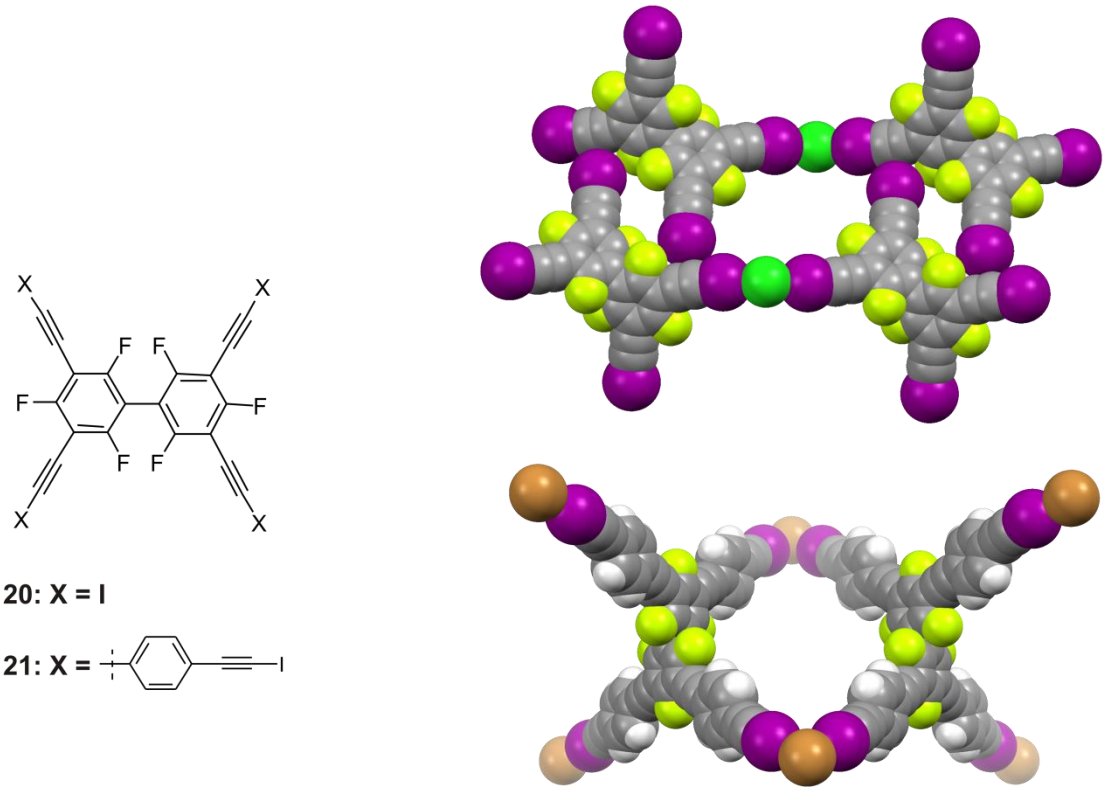

FIGURE 10 Schematic presentation of ligands **20** and **21** and crystal structures of insulating materials formed are presented in space filling mode (CSD ref. code: SIVYEC, DAKVAO).[80,81]

Crystallization of 1,3,5-tris(iodoethynyl)-2,4,6-trifluorobenzene **22** with halide salts with different size cations resulted in the formation of a variety of supramolecular anion organic frameworks (figure 11).[82] Similar to tritopic donor **3**[50], the anticipated (6,3) honeycomb-like networks were formed in cocrystallization of **22** with a 1:1 ratio of several halide salts. Large cavities formed within (6,3) networks were filled with cations and solvent and/or by up to 4-fold interpenetration. The most striking example of the formed architectures is the cocrystallization of **22** with $Et_3BuN^+Br^-$ in a 2:1 ratio. Unprecedented octahedral geometry around the bromide anion resulted in a halogen-bonded cubic structure, where the bromide anion behaves as a hexadentate XB acceptor towards six different molecules of **22**.

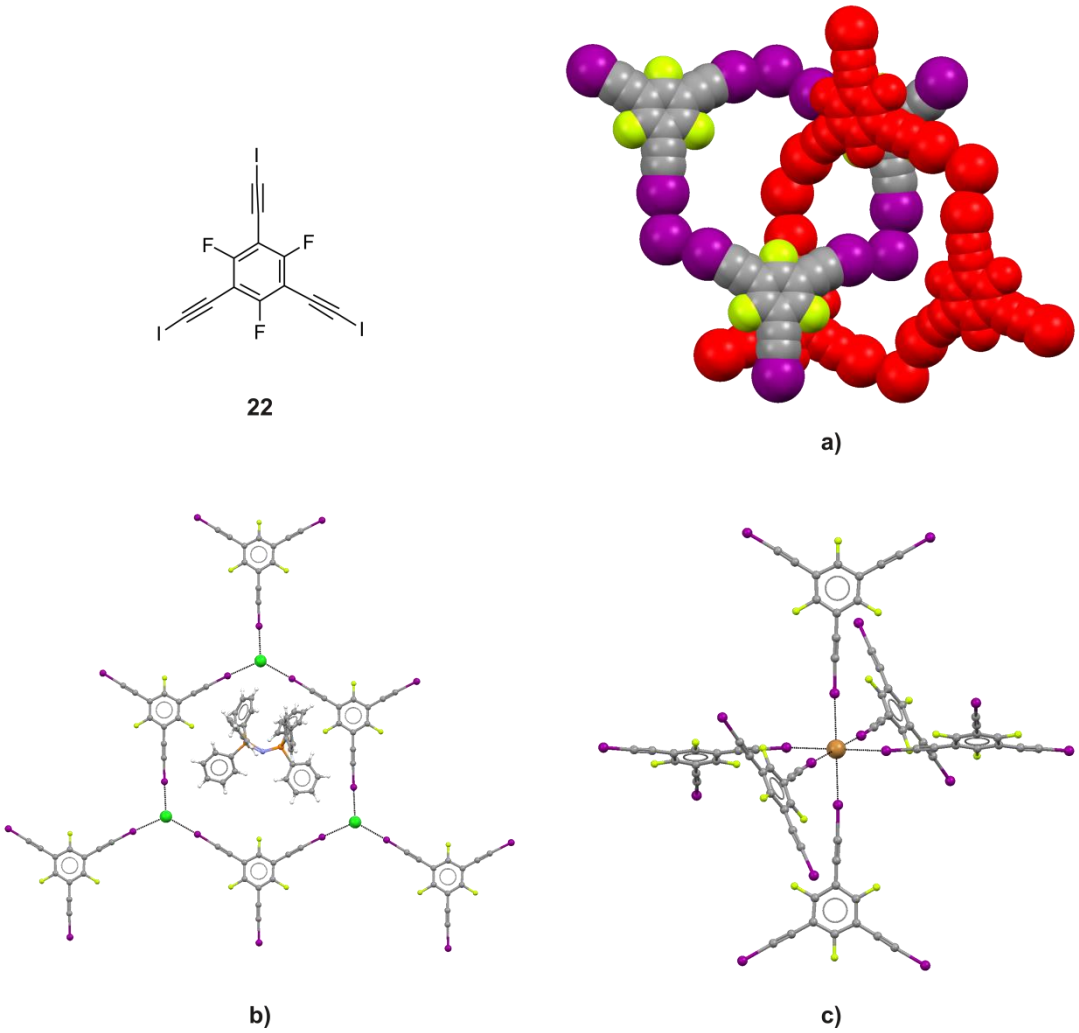

FIGURE 11 Structure of **22** and crystal structures of XB complex of **22** and a) Bu_3S^+ I^- presented in space filling mode, b) PPN^+ Br^- and c) Et_3BuN^+ Br^- (CSD ref. code: IFOJAQ, IFIGAH, IFANAG).[82]

1.1.3.3 N-X donors

N-Halosuccinimides are commonly used halogenating agents in synthetic organic chemistry. Even though halosuccinimides are known to interact with halides[83–85] and *N*-donors[86], it was only recently that the potential of the polarized N-X moieties to behave as XB donors was recognized.[87,88] One of the most interesting examples of *N*-iodosuccinimide (NIS) acting as a XB donor is a tetrahedral complex of NIS and hexamethylenetetramine (HMTA) (figure 12).[87] Interestingly, $[NIS]_4 \cdots [HMTA]$ complexes were stacked as columns that further formed cylindrical channels. The channels were stabilized by multiple weak C–H $\cdots$ O=C hydrogen bonds between HMTA or NIS and amide oxygen atoms of neighboring $[NIS]_4 \cdots [HMTA]$ complexes. Furthermore, changes in the shape and volume of the channels were observed depending on the solvent guest used.[88]

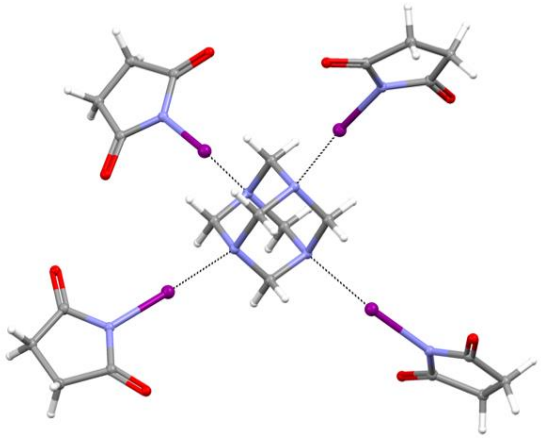

FIGURE 12 Crystal structure of the $[NIS]_4 \cdots [HMTA]$ complex (CSD ref. code: IBIZAW)[87]

Dolenc and Modec reported a series of complexes of *N*-halosaccharins with nitrogen and oxygen electron-pair donors.[89] Recently, *N*-iodosaccharin (NISac) was described as a strong XB donor by Fourmigué and co-workers.[90] The degree of the ionicity of the NIS and NISac XB complexes was estimated by measuring the position of the iodine atom in $A{-}I \cdots B \leftrightarrows [A]^- \cdots [I{-}B]^+$ systems. The XB complexes of NIS with pyridine, 4-methylpyridine, and 4-dimethylaminopyridine were described as close-to-neutral co-crystals, while in NISac · Py-NMe_2 complex the $I \cdots N$ bond was found to be shorter than the N−I bond of NISac, hence suggesting a "close-to-ionic" salt structure.[90] Similarly, very strong $^-N{-}X^+ \cdots {}^-O{-}N^+$ halogen bonds were found between NISac and *N*-oxides in solution and in the solid state.[91]

Fourmigué and co-workers used a ditopic N-I donor, *N,N'*-diiodo-dimethylhydantoin **23**, to study the effect of sequential XB formation.[92] Co-crystallization of **23** with electron-rich pyridines yielded XB bis-adducts, whereas mono-adducts were favored with electron-poor pyridines (figure 13). Crystallization studies of 2:1 adducts revealed some general trends in XB ability of **23**: i) shortest XB was found at the imidic iodine and slightly longer, yet still very short, XB at amidic iodine, ii) halogen bond strenghtening was observed by increasing the Lewis basicity of the pyridine (R = H, Me, NMe_2, NC_4H_8). In 1:1 adducts, the formation of XB between imidic iodine and pyridine lead to the deactivation of the amidic iodine. Thus, other XB acceptors were able to compete favorably with pyridine and chain-like structures were formed rather than 2:1 adducts.

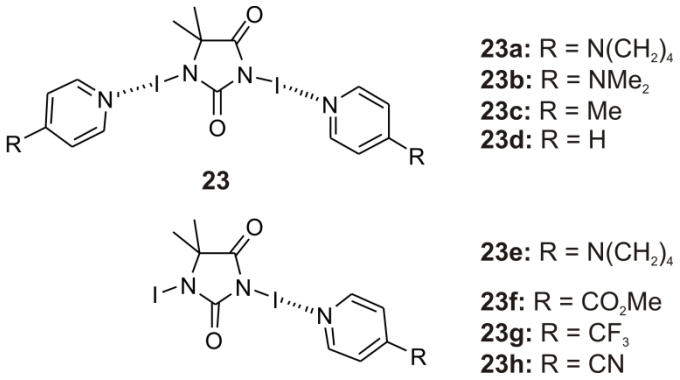

FIGURE 13 Schematic presentation of mono- and bis-adducts formed between **23** and pyridine derivatives.[92]

1.1.3.4 Imidazole- and triazole-based XB donors

Interactions between halogenated imidazole- and triazole-based moieties with halide anions have been especially exploited in studying halogen-bonded systems in solution. For this purpose, Beer and co-workers synthesized macrocyclic bidentate imidazoliophane receptors and studied their halide-anion recognition through halogen bonding.[93,94] Compared to hydrogen-bonding analogues, significantly enhanced halide-binding affinities of the XB receptors were observed in a competitive aqueous methanolic solvent.

Schubert and co-workers utilized halotriazole-based moieties in the synthesis of bidentate XB anion receptors and characterized their binding affinities in solution and in the solid state.[95,96] Compared to receptor **24**, receptor **25** is rigidified due to the intramolecular HBs, which results in significantly higher binding affinity towards Cl^- and Br^- (figure 14).[96] Also, isothermal titration calorimetry experiments in THF revealed that receptor **25** forms 1:1 and 2:1 complexes simultaneously with both halide anions.

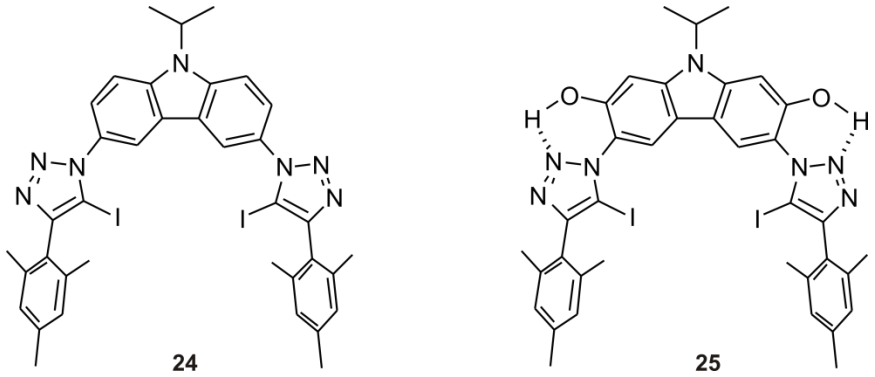

FIGURE 14 Structures of anion receptors **24** and **25**.[95,96]

Beer and co-workers utilized halogen bonding further as a directing interaction in the assemblies of interpenetrated molecular systems.[97–100] Halogen bonding was found to enhance the strength of anion-templated formation of pseudorotaxanes[97] and rotaxanes[98], even in water[100]. The crystal structure of anion-templated rotaxane **26** confirmed that the bromide is encapsulated within

the rotaxane's interlocked binding cavity by two complementary hydrogen and one halogen bonding interaction (figure 15).[98]

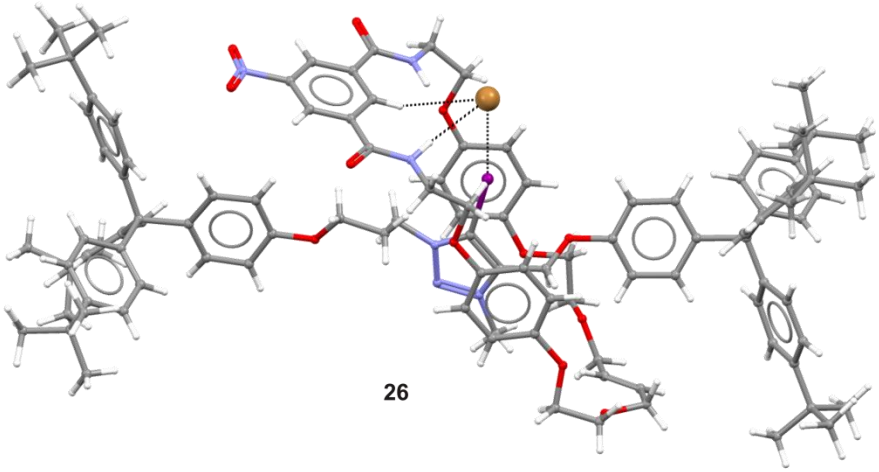

FIGURE 15 Crystal structure of the XB rotaxane **26** (CSD ref. code: TACPUK).[98]

1.1.4 Halogen-bonded capsular assemblies

One of the intriguing subclasses of multivalent halogen-bonded architectures are the capsular assemblies. To obtain capsules that are solely based on halogen bonds is a challenging task. As XBs are highly directional, correct design of donor and acceptor moieties is the key step in the construction of discrete capsular assemblies. Resorcinarenes and its derivatives have been shown to be useful building blocks in the construction of capsular assemblies through weak interactions.[101,102] Subsequently, resorcinarene frameworks have also been utilized in halogen-bonded capsules.

First pursuits towards halogen-bonded capsules were reported in 2012.[103] Self-assembly of a rigid methylene-bridged tetrakis(4-pyridyl)cavitand **27** with 1,4-diiodotetrafluorobenzene **15** in an acetonitrile/ethanol mixture yielded a halogen-bonded network where cavitand **27** behaved as a tetradentate XB-acceptor and **15** as a bidentate XB donor (figure 16a). When XBs are formed between nitrogen atoms of **27** and four molecules of **15,** an extended concave assembly is formed. Due to the linearity of the XB-acceptor molecules, the iodine atoms are too far apart to match the orientation of four nitrogen atoms of a single cavitand **27**. Thus, desired capsule formation is hindered. Capsular design was pursued further and taking advantage of supramolecular ''chelating'' effect, the self-assembly of a rigid methylene-bridged tetrakis(3-pyridyl)cavitand **28** and a flexible tetrakis(4-iodotetrafluorophenyl)calix[4]arene **29** resulted in the formation of pseudo-capsular XB complex **28** ⋯ **29** (figure 16b).[103]

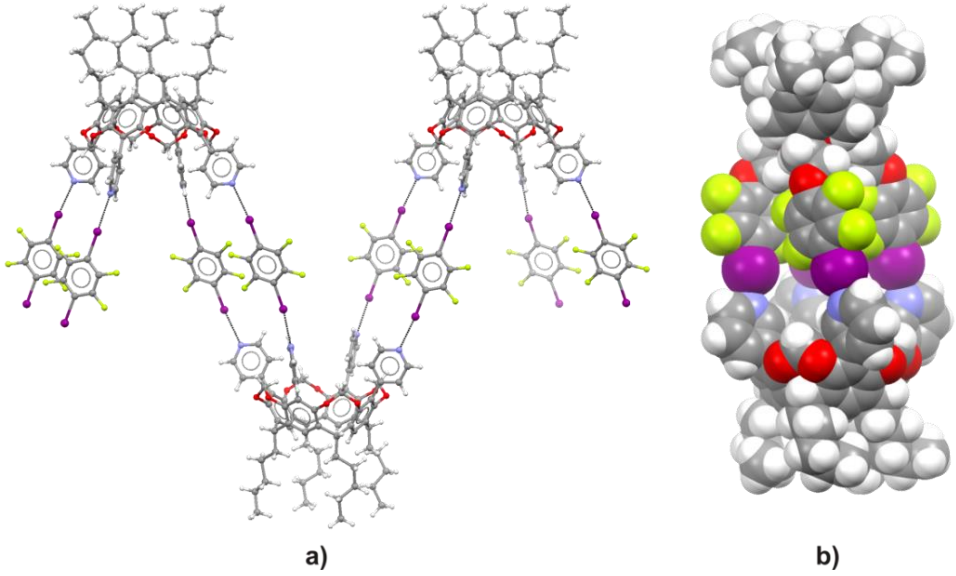

FIGURE 16 Crystal structures of a) cavitand-based XB network and b) XB pseudo-capsular dimer **28**···**29** presented in space filling mode (CSD ref. code: DEGWET).[103]

The halogen-bonded dimeric capsule **31** with a single cavity (V= 551 Å^3), large enough to encapsulate three 1,4-dioxane molecules, was achieved in the solid state by using *N*-alkyl ammonium resorcinarene salt **30** as XB acceptor and molecular iodine as bidentate XB donor (figure 17).[104] The capsule was composed of two molecules of **30** connected by two iodine molecules. Even though ^{1}H NMR spectroscopic studies confirmed the existence of iodine-to-resorcinarene salt halogen bonding, the dimeric capsule was not observed in solution due to the weakness of the second I···Cl$^-$ halogen bond. Resorcinarene salts were further used in the preparation of dimeric and capsular halogen-bonded assemblies with 1,4-diiodooctafluorobutane.[105]

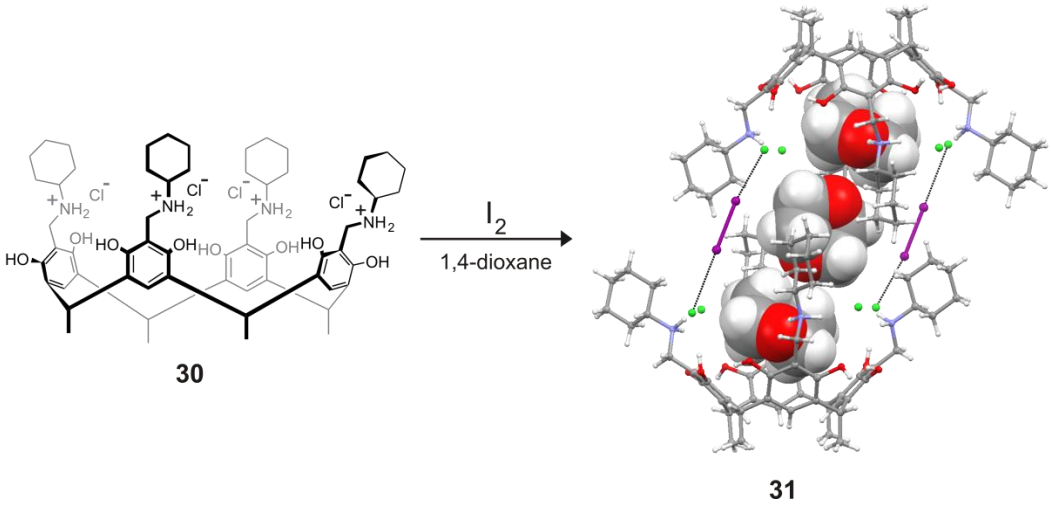

FIGURE 17 Formation and crystal structure of dimeric XB capsule **31** (CSD ref. code: CALJUX). Encapsulated dioxane molecules are presented in space filling mode.[104]

Diederich and co-workers reported halogen-bonded molecular capsules along with their host-guest binding properties in solution.[106] The XB capsules were obtained by using tetrafunctionalized cavitands with 2,3,5,6-tetrafluoro-4-halophenyl and pyridyl moieties. The capsule formation was followed by ^{19}F NMR spectroscopy in deuterated benzene/acetone/methanol (70:30:1) mixture. This solvent mixture was needed to fully solubilize all the compounds and furthermore, a minimum amount of methanol was found to be crucial for preventing the flapping of the benzimidazole walls. Capsule formation was realized for donors containing I and Br, but not for F and Cl derivatives. Subsequently, X-ray crystal structure of the neutral XB capsule **32** was reported (figure 18).[107] The reported assembly consisted of 12 components with two cavitands, geometrically rigidified by hydrogen bonding to eight methanol molecules, forming a halogen-bonded capsule that encapsulated two benzene molecules.

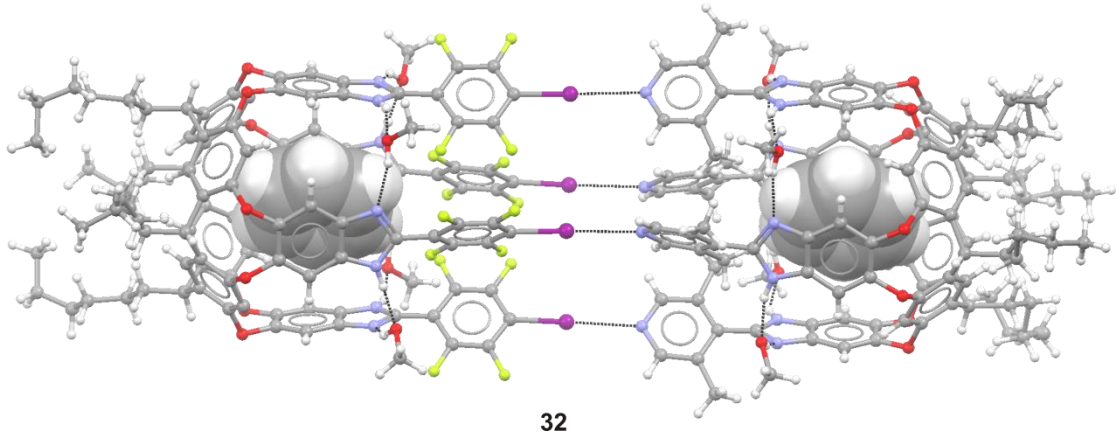

32

FIGURE 18 Crystal structure of XB capsule **32** (CSD ref. code: IBUZEN). Encapsulated benzene molecules are presented in space filling mode.[107]

To investigate the influence of different XB donor and acceptor moieties on capsule formation, iodoethynyl(tetrafluorophenyl) and quinuclidyl residues were attached to the benzimidazole walls.[107] The structural modifications were anticipated to enhance the capsular association strength. However, all experiments resulted in precipitation or degradation of the compounds. Also, as evidenced by crystal structure, the quinuclidyl cavitand was found to form hydrogen bonds with methanol, thus hindering the desired capsule formation. Finally, iodoethynyl(tetrafluorophenyl) cavitand **33** was found to strongly bind with lutidyl cavitand **34** resulting in the formation of dimeric XB capsule **33**$\cdots$**34** with the highest affinity among the molecules investigated.[107]

1.2 Halonium ions

In the last section of this literature review, halogen-bonded complexes involving halonium ions are discussed. Halonium ions are R_2X^+-formed cations that consist of a halogen atom (X = F, Cl, Br, I) bound to two organic residues. The halogen atom bears a formal charge of +1 and it is therefore a highly reactive electrophilic species that readily reacts with nucleophiles. Halonium ions have gained considerable attention due to their behavior as intermediates in organic syntheses, *e.g.* in electrophilic addition to alkenes, but their role in halogen bonding has received less attention.

The fundamental problem of systems containing halonium ions is the nature of the chemical bond of these complexes. The definition of the XB includes systems with X^+ cations where interactions are mainly electrostatic. However, problems arise when the interaction of the system has considerable covalent nature and terms coordinative halogen bond or halogen bond with coordinative nature have been suggested.[108] From this perspective R_2X^+ systems could be seen as special cases of XB. Accordingly, halonium ions are the strongest halogen bond donors known so far.

Throughout this thesis the term '[N···X^+···N] halogen bond' is used to describe a supramolecular synthon where the halonium ion (the halogen bond donor) forms two simultaneous X^+···N halogen bonds to two nitrogen-containing XB acceptors.

1.2.1 [N···X^+···N] halogen bond

The existence of Py_2I^+ cations was confirmed by single-crystal X-ray diffraction studies in 1961.[109] The crystal structure revealed a centrosymmetric arrangement of Py_2I^+ with I_3^- as a counteranion. Subsequently, several X-ray structures involving nitrogen moieties and iodonium or bromonium ions have been reported, but they were mainly studied as charge-transfer complexes or reactive intermediates in organic synthesis.[110–116] In general, [N···X^+···N] systems were found to be fully or close to symmetric with the bond angle near 180°. Pyridine and pyridine derivatives are commonly used in the formation of linear [N···X^+···N] bonds, and crystal structures containing I^+ and Br^+ but no Cl^+ or F^+ ions have been reported.[111,116,117] [N···X^+···N] bonds containing other than aromatic sp^2 nitrogen atoms are also known.[110, 113,118] As a representative example of three-center four-electron [N···X^+···N] complexes, bis(pyridine)iodonium tetrafluoroborate **35**, also known as Barluenga's reagent, has found applications as a mild iodinating and oxidizing reagent (figure 19).[119]

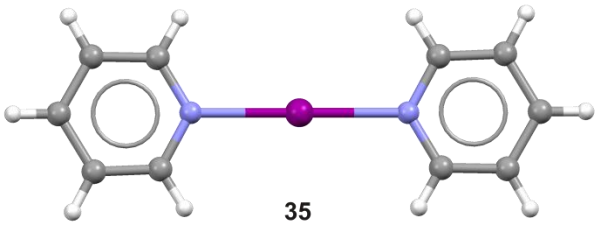

FIGURE 19 Crystal structure of bis(pyridine)iodonium tetrafluoroborate **35**. The counteranion BF_4^- has been omitted for clarity (CSD ref. code: HUMMAD).[120]

Halonium ions were first studied from the perspective of halogen bonding by Erdélyi and co-workers.[121–126] In these three-center four-electron (3*c*4*e*) [N···X⁺···N] systems, a halonium ion (X^+) is simultaneously stabilized by two identical nitrogen electron donors, pyridine or pyridine derivatives (figure 20). In such systems the halonium ion can either be centered between nitrogen atoms or be closer to one nitrogen atom making the system asymmetric. In a symmetric arrangement X^+ is centered between two donors with equally strong and long N···X bonds. Generally, the formation of symmetric 3*c*4*e* bond systems results in a significant stabilization due to the comparable orbital and electrostatic contributions and a large extent of charge delocalization. In an asymmetric system there is one shorter and stronger covalent N-X bond and one longer and weaker N···X halogen bond.[127]

The [N···X⁺···N] halogen bond and the [N···Ag⁺···N] coordination bond are structurally analogous. Both systems result in bis-coordinated 3*c*4*e* complexes with linear geometry and are generally compared with each other.[108]

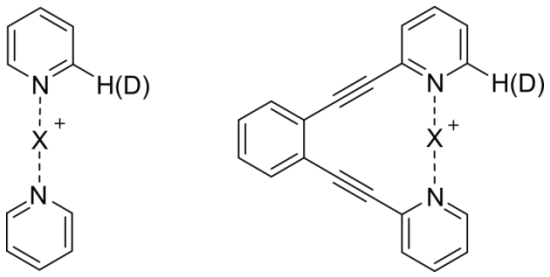

FIGURE 20 Structures of [bis(pyridine)iodine]⁺ complexes used to investigate 3*c*4*e* systems in solution and in solid state.[121]

Detailed studies of the geometry of the [N···X⁺···N] systems in solution were carried out by NMR spectroscopic and computational methods.[121,122] Comprehensive results on [bis(pyridine)halonium]⁺ and geometrically restrained [1,2-bis(pyridine-2-ylethynyl)benzenehalonium]⁺ complexes showed that bromine(I) and iodine(I) preferred static symmetric arrangements in solution (figure 20).[121,122] The existence of analogous Cl^+ and F^+-complexes was also proven by NMR and computational methods.[124] The [N···Cl⁺···N] systems were found to be weaker than the analogous Br^+ and I^+ complexes and they

similarly preferred a symmetric arrangement, whereas [N···F⁺···N] was found to prefer an asymmetric arrangement.

The stability of the symmetric 3*c*4*e* bonds was systematically studied by altering the environment and electronic properties of the system.[123,125,126] Solvent effects to model systems, bis(pyridine)halonium triflates, were studied in dichloromethane (CH_2Cl_2) and acetonitrile (CH_3CN).[123] CH_2Cl_2 should not interact with [N···X⁺···N] systems, whereas CH_3CN is a Lewis base competing with pyridine for coordination to X⁺. It was shown that polar, aprotic CH_3CN is unlikely to interact with the halonium ion and hence unable to destabilize the 3c4e bond. However, due to its polarity, CH_3CN was found to slightly modulate the energy of the interactions as well as the solubility of the counterion.

The influence of the counterions on the symmetries of [N···I⁺···N] XB systems and [N···Ag⁺···N] coordination complexes was studied in solution and the solid state.[125] Anions of varying size, charge distribution and coordination strength were investigated. Results showed the coordination strength of the counterions does not influence the geometry of [N···I⁺···N] halogen bond either in solution or in the solid state. However, the coordination strength of the counteranion was found to influence the linearity and occasionally the symmetry of the [N···Ag⁺···N] coordination bond (figure 21).

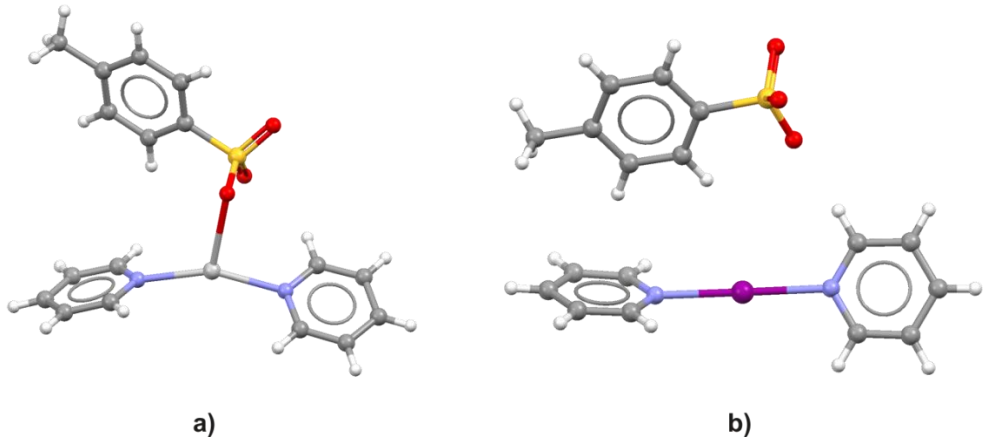

FIGURE 21 Crystal structures of bispyridine complexes with a) silver tosylate and b) I⁺ showing the counterion influence on the [N···Ag⁺···N] and [N···I⁺···N] bonds (CSD ref. codes: LULBEB, LULBIF).[125]

The influence of electron density alteration on the strength and geometry of [N··· I⁺···N] halogen bond was systematically studied by spectroscopic and computational methods.[126] [Bis(pyridine)iodine]⁺ and [1,2-bis((pyridine-2-ylethynyl)benzene)iodine]⁺ BF_4^- complexes were substituted with electron withdrawing and donating groups (NO_2, CF_3, H, F, Me, OMe, NMe_2) in the *para*-position of their pyridine N-atoms. It was expected that the decreased electron-donating ability of the nitrogens would destabilize the symmetric [N··· I⁺···N] halogen bond and increase the reactivity of the complex. On the other hand, by increasing the electron density, the stabilization of the symmetric [N···I⁺···N] geometry by strengthening the two N···I halogen bonds and

thus, decreasing the reactivity of the complex was expected. It was observed that an increased electron density of the pyridyl moieties stabilizes the halogen bond, whereas decreasing the electron density reduces the stability of the complexes. Interestingly, changes in electron density did not significantly affect the symmetric geometry or the bond lengths of the [N···I⁺···N] halogen bond in solution or in the solid state.

1.2.2 3*c*4*e* bonds with sulphur and selenium

Sulphur and selenium are also able to form 3c4e bonds with halonium ions. However, they are less studied and only structures with iodine(I) are known so far.[108,128–137] Crystals grown from a 2:1 mixture of thiourea and iodine revealed the formation of bis(thiourea)iodine(I) cations **36**, which is the first example of [S···I⁺···S] systems in the solid state (figure 22).[128]

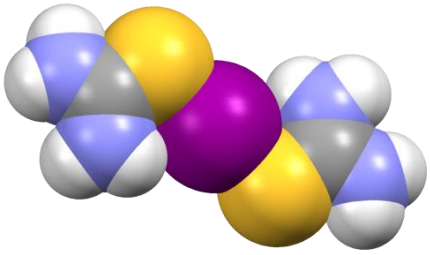

36

FIGURE 22 Crystal structure of bis(thiourea)iodine(I) complex **36**. Counterions are omitted for clarity (CSD ref. code: ISUREA10).[128]

Recently, unexpectedly strong I⁺···S halogen bonds were observed when 2-imidazolidinethione and I_2 were mixed in CH_2Cl_2.[108] The formation of a charge-transfer complex 2-imidazolidinethione-2(I_2) **37** was followed by a heterolytic cleaveage of a diiodine, which resulted in the formation of I⁺ along with the counterions I^- and $[I_3]^-$. The [S···I⁺···S] halogen bond in the iodonium complex $[I(2\text{-imidazolidinethione})_2]^+ \cdot 1/2I^- \cdot 1/2[I_3]^-$ **38** was observed not to be only an electrostatic contact but it had a dual nature with considerable coordinative nature.[108]

[Se···I⁺···Se] complexes also show structural features similar to other 3*c*4*e* bond analogues.[134–137] The bond angles in [Se···I⁺···Se] systems are generally close to 180° and the bond distances are shorter than the respective van der Waals radii. The first example of such a system was achieved by adding a slight excess of iodine to a 1:1 mixture of $^tBu_3PSe$ and I_2, which caused a transition from $^tBu_3PSeI_2$ to the cationic $(^tBu_3PSeI)^+$ complex **39** (figure 23).[135]

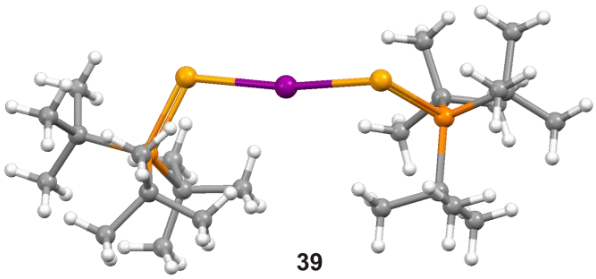

FIGURE 23 Crystal structure of $(R_3PSe)_2I^+$ complex **39**. Counterions are omitted for clarity (CSD ref. code: DIJYUQ).[135]

2 RESULTS AND DISCUSSION

2.1 Aim of the Work

The aim of the work was to synthesize multivalent halogen bond donor and acceptor molecules and study their utilization in halogen-bonded supramolecular assemblies, capsules and cages. Upper rim tetrafunctionalized resorcinarene cavitands were chosen as core frameworks due to their concave and preorganized structures. Rigid methylene- or more flexible ethylene-bridged cavitands were used as platforms for haloacetylene donors. The behaviour of the preorganized tetravalent donor molecules towards neutral and anionic XBs was studied mainly in the solid state by single-crystal X-ray crystallography.[I,V]

The [N···Ag$^+$···N] → [N···I$^+$···N] cation exchange reaction was applied in the construction of [N···I$^+$···N] halogen-bonded capsules and cages.[II-IV] Ethylene-bridged tetrakis(pyridyl)cavitands were used in the formation of [N···I$^+$···N] halogen-bonded capsular assemblies through their analogous silver(I) coordination complexes.[II,III] Depending on the position of the pyridine N-atoms, either dimeric or hexameric capsules were achieved. Utilization of [N···I$^+$···N] halogen bonds to construct supramolecular architectures was further studied with tripodal *N*-donors.[IV] The [N···I$^+$···N] halogen-bonded assemblies were studied in solution with nuclear magnetic resonance spectroscopy (NMR), in the solid state with single-crystal X-ray crystallography and in the gas phase with mass spectrometry.

2.2 Syntheses

2.2.1 Synthesis of cavitand framework[I,II,III,V]

Cavitand frameworks with different lower rim alkyl chains and methylene or ethylene bridging groups were synthesized in three steps from resorcinol according to the reported procedures (scheme 1).[138–141] In the first step resorcinarene was formed in an acid-catalysed condensation reaction between resorcinol **40** and aldehyde **41**. Hexyl and isobutyl chains were introduced to the lower rim due to their different solubilities and crystallization behaviour. Resorcinarene syntheses were followed by halogenation reactions, where resorcinarene **42** was stirred at room temperature from 3h to overnight either with *N*-bromosuccinimide (NBS) in 2-butanone or with elementary iodine in a 1:1 mixture of water and diethyl ether in the presence of K_2CO_3. In halogenation reactions the products **43-46** precipitated out as white solids. In the next step halogenated resorcinarenes **43-46** were stirred with either bromochloromethane or 1-bromo-2-chloroethane and K_2CO_3 in dry dimethylformamide (DMF) under argon for 24h at 40°C and then for 48h at 80°C. Subsequent work up and column chromatography afforded the methylene- and ethylene-bridged cavitands **47-51** as white solids in yields of 46-63%.

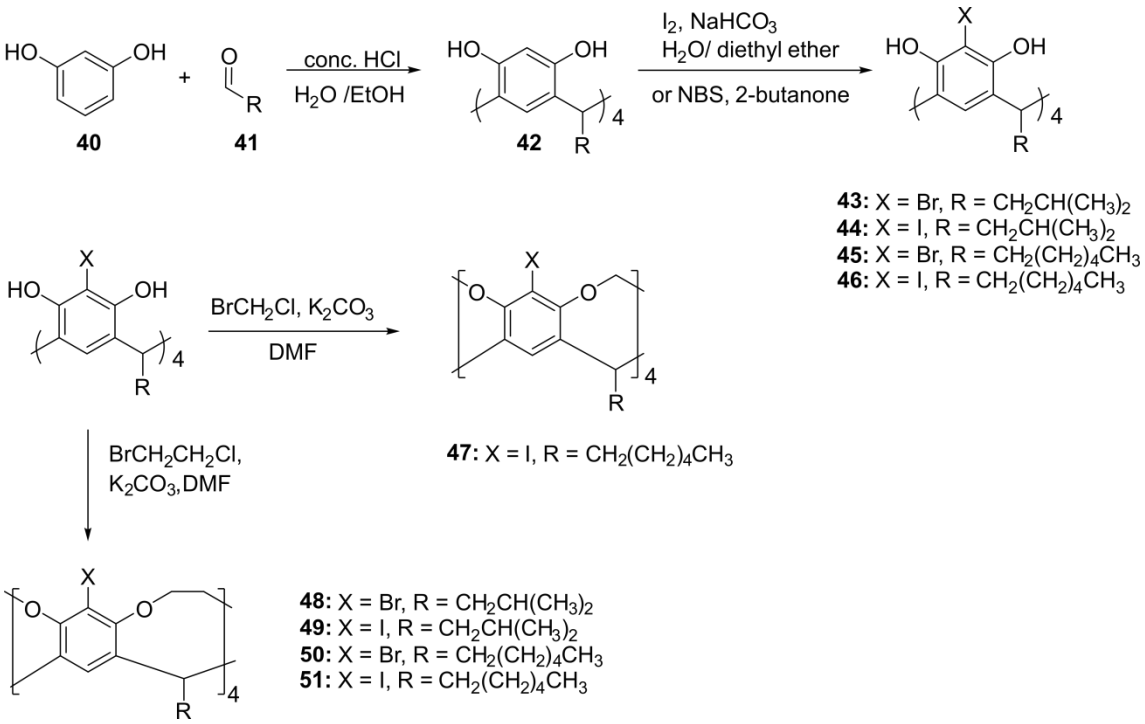

SCHEME 1 General synthesis route of the cavitand frameworks.

2.2.2 Syntheses of XB donors[I,V]

Haloethynyl groups were introduced to the methylene- or ethylene-bridged cavitand framework in two steps by following modified reported procedures (scheme 2).[82,142–144] Tetraiodocavitand **47** or **51**, [$Pd(PPh_3)_4$], copper(I) iodide and ethynyltrimethylsilane in dry triethylamine were refluxed at 100°C for 18 h. Work up and column chromatography afforded the tetra[(trimethylsilyl)ethynyl] cavitands **52** and **53** as white precipitates in yields of 47-84%. Sonogashira cross-coupling reactions were followed by the final halogenation steps. Cavitands **52** and **53** were treated with *N*-iodosuccinimide (NIS) in the presence of silver fluoride in acetonitrile to give the tetraiodoethynyl cavitands **54** and **56** as white solids in yields of 44-96%. Analogous tetrabromoethynyl cavitand **55** was prepared by following the same procedure with *N*-bromosuccinimide (NBS).

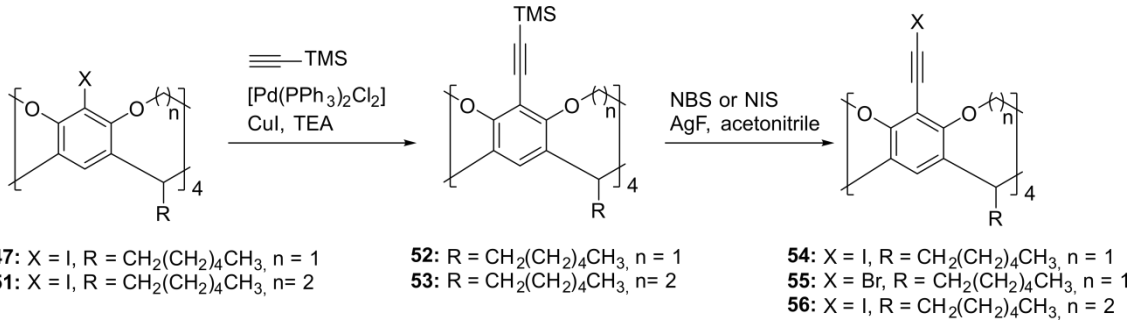

SCHEME 2 General synthesis route of the haloethynyl cavitands.

2.2.3 Designing XB acceptors for [N···I⁺···N] halogen-bonded capsular assemblies[II,III]

In the construction of [N···I⁺···N] halogen-bonded supramolecular dimeric and hexameric capsules, the correct design of the nitrogen-containing acceptors plays important role as the [N···I⁺···N] bond angle is close to 180° limiting the structural flexibility of the system. Therefore, utilization of multiple linear [N···I⁺···N] halogen bonds in the formation of such assemblies would be feasible by using spatially preorganized acceptor ligands.

The [N···I⁺···N] halogen-bonded dimeric and hexameric capsules can be synthesized from the structurally analogous [N···Ag⁺···N]-bridged metallo-supramolecular capsules by applying the [N···Ag⁺···N] → [N···I⁺···N] cation exchange reaction.[115] Therefore, the monomer has to be sufficiently rigid and possess suitable curvature and directionality of multiple binding sites to produce selectively the silver-coordinated dimeric and octahedral hexameric capsules. However, to be able to form multiple linear [N···Ag⁺···N] or [N···I⁺···N] bonds, the monomer should also be flexible enough to tolerate small differences from the ideal geometry. This is not possible with the methylene-bridged resorcinarene cavitand because, based on molecular modelling, the short methylene-bridges rigidify the four resorcinolic benzene rings so that the angle

between the opposing rings is 64° (figure 24, A). This angle is too small for the formation of dimeric or octahedral hexameric capsules through pyridine N-atoms in *meta*- or *para*-position.

Instead, the corresponding ethylene-bridged cavitands satisfy much better the structural requirements for the formation of [N···Ag^+···N] and [N···I^+···N]-bridged dimeric and octahedral hexameric capsules. Therefore, ethylene-bridged tetrakis(3-pyridyl)cavitand can be used in the construction of the dimeric capsules, as the pyridine N-atoms are in positions that enable, with a slight helical twisting, connecting two cavitands with a linear linker.

Based on molecular modelling, in the ethylene-bridged tetrakis(4-pyridyl)cavitand, the angle between the opposing rings is very close to 90° (figure 24, B). Therefore, connecting the ethylene-bridged tetrakis(4-pyridyl)cavitands through linear [N···Ag^+···N] and [N···I^+···N] binding motifs should result in the formation of octahedral hexameric capsules.

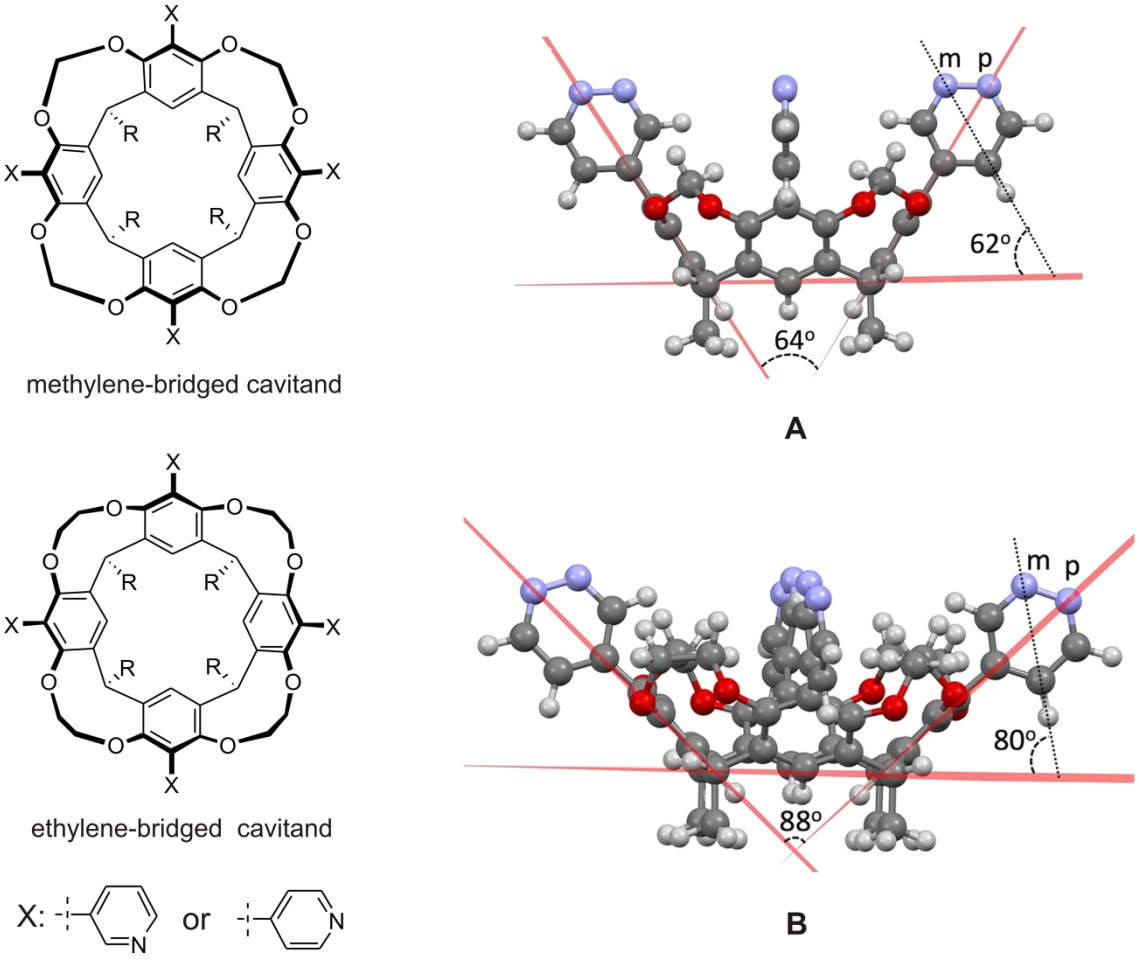

FIGURE 24 Schematic presentation of the design of the pyridine-based donors to produce the required geometry.

2.2.4 Syntheses of XB acceptors[II,III,IV]

Pyridine-based acceptor molecules were synthesized by fourfold Suzuki coupling of 3- or 4-pyridylboronic acid to ethylene-bridged tetraiodo- or tetrabromocavitands **48-51** (scheme 3).[116,II] In general, halogenated ethylene-bridged cavitand **48-51**, pyridyl-3/4-boronic acid, [$Pd(PPh_3)_4$] and Cs_2CO_3 (2.0 g, 6.3 mmol) in degassed 1,4-dioxane and water mixture were refluxed at 110 °C for 2 d. Subsequent work up and column chromatography afforded the products **57a,b** and **58** as white solids in yields of 38-50%.

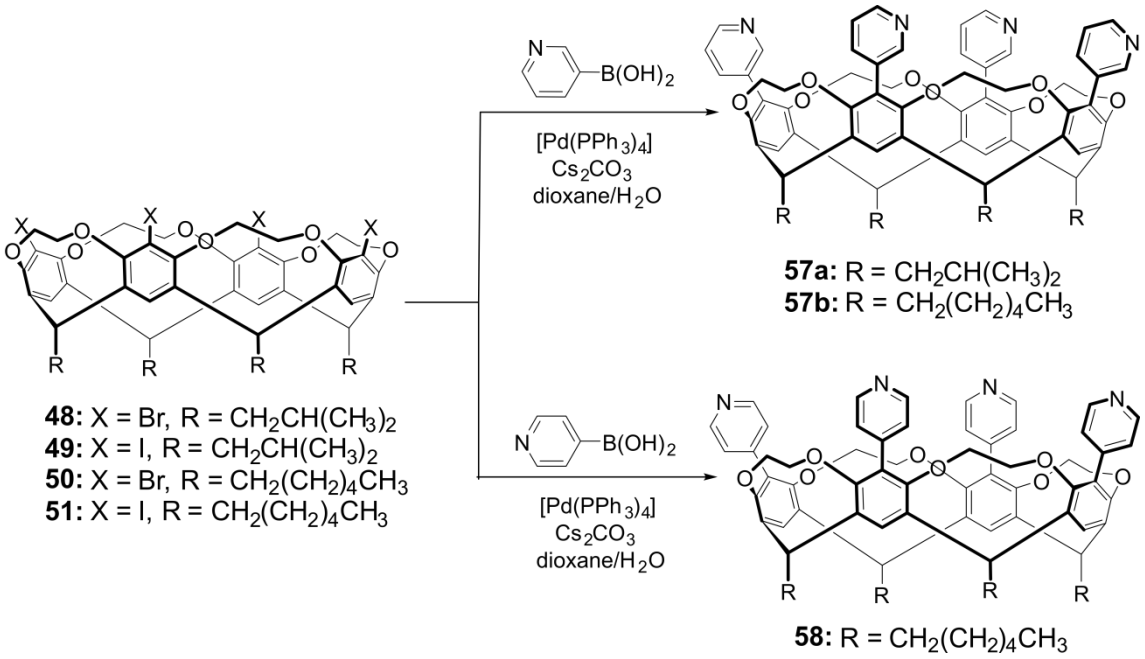

SCHEME 3 Synthesis route for the ethylene-bridged tetrakis(pyridyl)cavitands.

Tripodal acceptor ligands **60** and **61** were synthesized according to reported procedures (scheme 4).[146,147] Ligand **60** is formed in a reaction between DABCO and 2,4,6-tris(bromomethyl)mesitylene **59** in acetonitrile followed by an anion exchange reaction where the bromide counterions are replaced by less coordinating hexafluorophosphate (PF_6^-) anions. A reaction of imidazole and **59** under basic conditions in dry DMF resulted in the formation of ligand **61**.

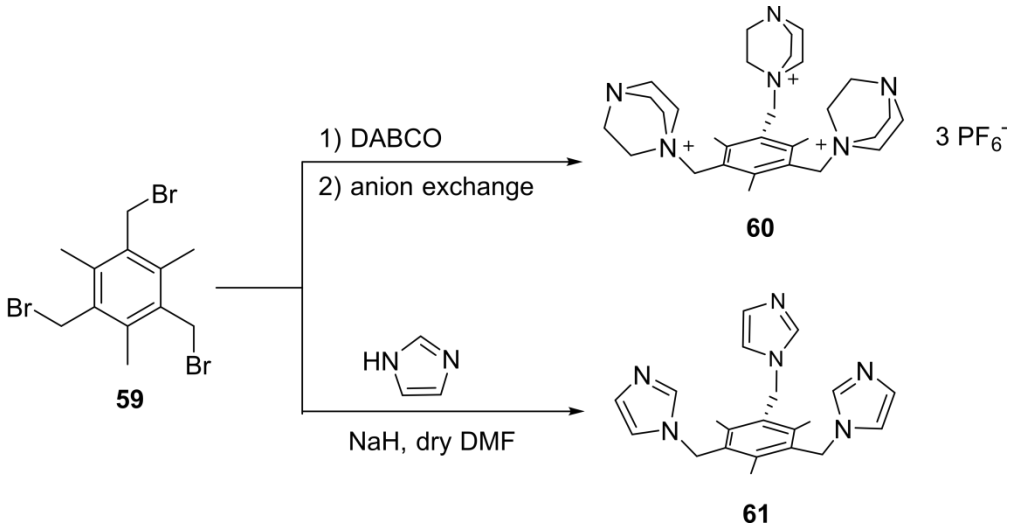

SCHEME 4 Synthesis route for the ligands **60** and **61**.[146,147]

2.2.5 Syntheses of [N···I⁺···N] halogen-bonded complexes[II,III,IV]

The commonly used procedure to prepare [N···I⁺···N] halogen-bonded species is to first synthesize the structurally analogous [N···Ag⁺···N] coordination complex.[115] Subsequent [N···Ag⁺···N] → [N···I⁺···N] cation exchange reaction should result in the formation of [N···I⁺···N] halogen-bonded species. Bis-coordinated three-center four-electron pyridine-based complexes of Ag^+ and I^+ exhibit linear geometry.[108,125]

In general, ethylene-bridged tetrakis(pyridyl)cavitands **57** and **58** or ligands **60** and **61** were stirred with silver(I)salts in either dichloromethane, chloroform or acetonitrile at room temperature for 10 min. The formation of Ag^+-coordination complexes was confirmed in solution by NMR measurements (^{1}H NMR, ^{1}H DOSY), in gas phase by ESI-MS and when X-ray quality crystals were obtained, in solid state by single-crystal X-ray crystallography.

The addition of molecular iodine to the solution of Ag^+-complexes led to the immediate precipitation of AgI and *in situ* formation of I^+ followed by the formation of [N···I⁺···N]-bridged complexes. The complexes were confirmed in solution by ^{1}H NMR, ^{1}H DOSY and ^{1}H, ^{15}N-HMBC measurements. The formed complexes were further characterized in the gas phase by ESI-MS. Single-crystal X-ray crystallography was used to determine the solid-state structures of [N···I⁺···N] halogen-bonded cages.

No specific conditions were needed during the complexation experiments, thus highlighting the robustness of the [N···I⁺···N] halogen-bonded assemblies. The [N···Ag⁺···N] → [N···I⁺···N] cation exchange procedure was found to be very selective; in all cases only the desired [N···I⁺···N] halogen-bonded assembly was obtained.

2.3 Solid-state studies of haloethynyl cavitands[I,V]

Haloacetylenes have been used in solution and in solid state to create halogen-bonded architectures (section 1.1.3.2), but their utilization in the preparation of 3D architectures is less common. By attaching four haloacetylene groups to methylene-bridged cavitand a spatially preorganized multivalent XB donor with C_{4v} symmetry can be achieved. As haloethynyl cavitands are very rigid building blocks, various architectures can be prepared by using different XB acceptor molecules.

The halogen bonding ability of the haloethynyl cavitands was studied in the solid state by single-crystal X-ray crystallography. X-ray quality crystals, generally obtained by slowly evaporating a mixture of iodoethynyl cavitand **54** or **56** with neutral or anionic acceptors, confirmed the formation of XB complexes where cavitands behaved as multivalent XB donors.

Interestingly, the crystal structure of methylene-bridged cavitand **54** with 1,4-dioxane showed strong self-inclusion behaviour of the cavitands (figure 25). Slow evaporation of the 1,4-dioxane solution of the cavitand **54** resulted in the formation of a self-included dimeric assembly where one of the iodoethynyl-groups is located in the cavity of the second cavitand (figure 25b). The other three iodoethynyl-groups behave as XB donors and are halogen-bonded to the oxygen atom of the 1,4-dioxane. Two 1,4-dioxane molecules act as ditopic acceptors connecting two different cavitands, while the third 1,4-dioxane acts as a monotopic halogen bond acceptor.

A closer look at the crystal structure of the self-inclusion dimer revealed a pair of C-H···C≡C triple bond interactions; hence, the strong self-inclusion behaviour is probably due to the combined results of electrostatic forces and space compensation.

Similar dimerization behaviour was observed when cavitands **54** and **55** were crystallized as halogen-bonded solvates from acetone, chloroform, acetonitrile and DMF.

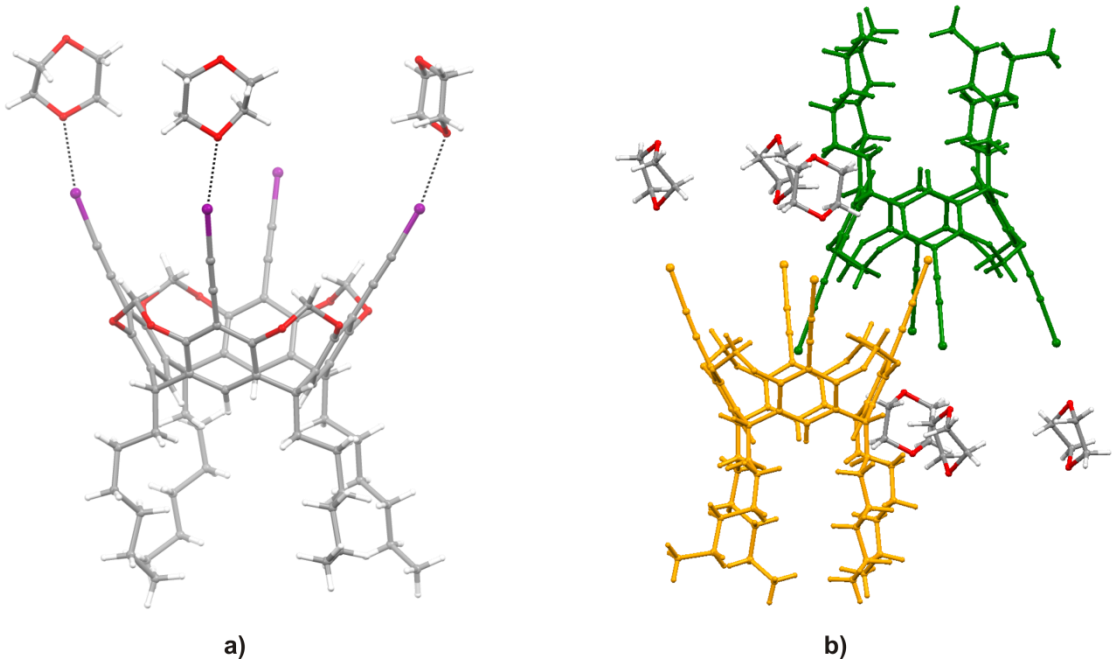

FIGURE 25 Crystal structure of **a) 54** · 1,4-dioxane without self-inclusion and **b)** the self-inclusion complex.

To prevent the strong self-inclusion behaviour of the XB donor molecules, the methylene bridge of the cavitand was changed to ethylene. Structural modifications were anticipated to hinder the formation of C-H···C≡C interactions and thus, free all four haloethynyl groups to form XBs. Also, an ethylene bridge would provide a slightly wider and more flexible framework compared to the methylene analogue.

Slow evaporation of the cavitand **56** from a pyridine solution resulted in the formation of an XB complex where all four iodine atoms were halogen-bonded to nitrogens of pyridine molecules (figure 26a,b). Similarly, an XB complex was obtained by slowly evaporating an acetone/$CHCl_3$-solution of cavitand **56** and an anionic acceptor, tetrapropylammonium bromide (TPA Br) (figure 26c). A halogen-bonded network structure was formed; in it all iodines behaved as XB donors and were halogen-bonded to bromide anions, which acted as bidentate acceptors.

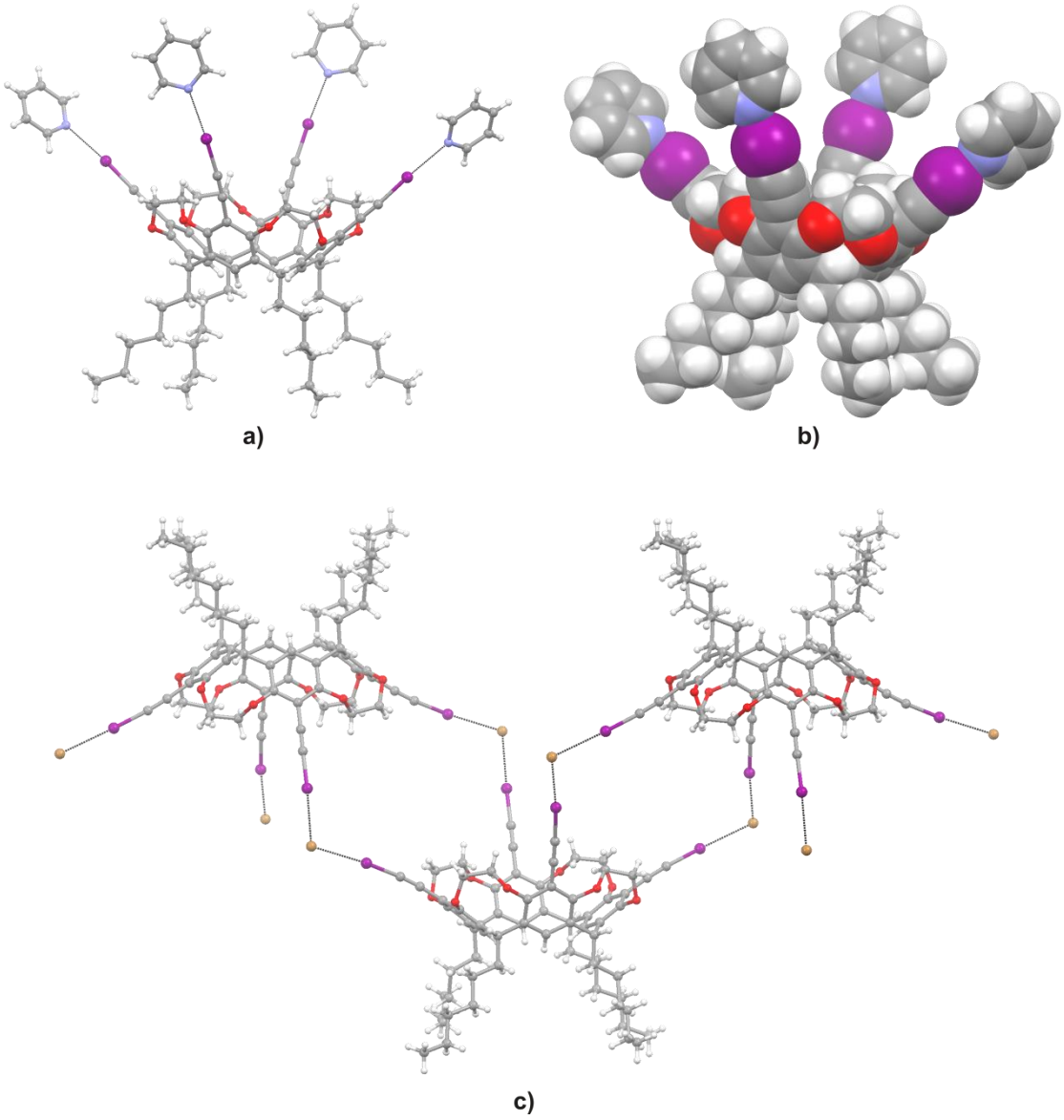

FIGURE 26 Crystal structures of a) **56** · pyridine in ball-and-stick mode, b) **56** · pyridine in space-filling mode and c) **56** · TPA Br. Counteranions and solvent molecules are omitted for clarity.

2.4 Cavitand-based metal-ligand coordinated and [N ··· I⁺ ··· N] halogen-bonded dimeric capsules[II]

The utilisation of multiple halonium ions in the formation of halogen-bonded assemblies was tested with ethylene-bridged tetrakis(3-pyridyl)cavitands **57a** and **57b**, which were expected to result in the formation of dimeric capsules (scheme 5).

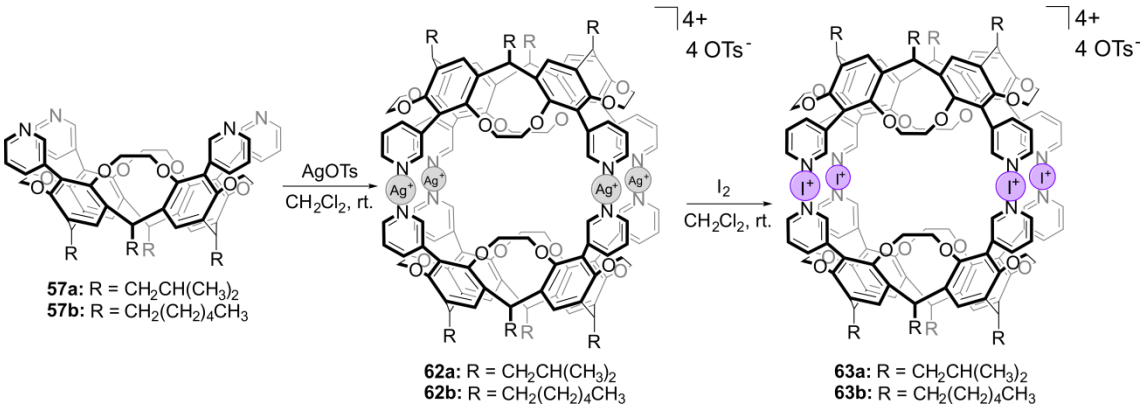

SCHEME 5 Synthesis of the [N···I⁺···N]-bridged dimeric capsule **63** through structurally analogous Ag^+-coordination complex **62**.

Somewhat surprisingly, ^{1}H NMR and ^{1}H DOSY measurements of the intermediate Ag^+-bonded dimeric capsules **62a** and **62b** resulted in complex spectra suggesting the formation of a mixture of species (figure 28b). Formations of more than one intact [N···Ag^+···N]-bridged capsules was further supported by the crystal structure obtained for Ag^+-capsule **62a** (figure 27). Single crystals of capsule **62a** were obtained by slow evaporation of DCM/ACN-solution of a 1:2 mixture of **57a** and AgOTs. Interestingly, the crystal lattice contains two structurally different centrosymmetric dimeric capsules. The difference between the capsules is due to the different Ag-coordination and the amount of coordinated water molecules, which results in slightly different cavity structures. Both capsules tightly entrap two dichloromethane molecules, but the volumes of the cavities were found to deviate from each other being 207 and 223 Å^3.

The ESI-MS spectra of capsules **62a** and **62b** showed dimeric complexes as the [**57a**$_2$·Ag_4·OTs_2]$^{2+}$ and [**57b**$_2$·Ag_4·OTs_2]$^{2+}$ ions at *m/z* 1512 and *m/z* 1624.

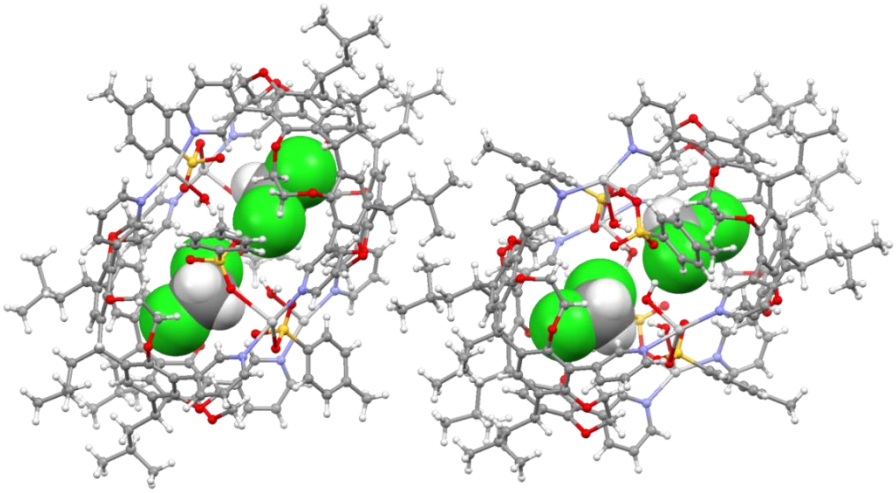

FIGURE 27 Crystal structures of the Ag^+-capsules **62a_a** and **62a_b**. Encapsulated CH_2Cl_2 molecules are presented in space-filling mode.

To obtain the [N⋯ I⁺ ⋯N] halogen-bonded dimeric capsules, molecular iodine was added to the 1:2 mixture of the cavitand **57a** or **57b** and AgOTs. After filtration of the precipitated AgI, ^{1}H NMR spectra were measured for I⁺-capsules **63a** and **63b**. Even though a mixture of species was obtained for the Ag⁺-capsules, the ^{1}H NMR spectra showed only one set of well-resolved signals indicating the formation of symmetrical [N···I⁺···N]-bridged capsules **63a** and **63b** (figure 28). All the pyridine proton signals were shifted downfield compared to the signals of the respective free cavitand supporting the formation of [N···I⁺···N] halogen bonds.

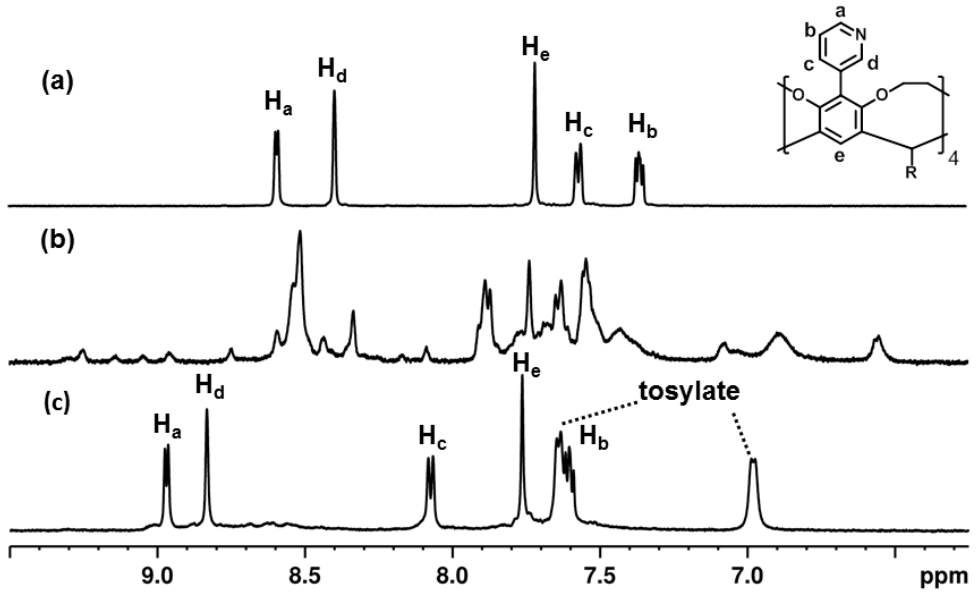

FIGURE 28 Aromatic region of the ^{1}H NMR spectra (CD_2Cl_2, 500 MHz, 298 K) of a) **57a**, b) **62a** and c) **63a.**

^{1}H DOSY measurements were made to obtain more information of the structures of the formed assemblies in solution. Measurements in dichloromethane at 298 K revealed one set of signals for both capsules **63a** and **63b** with diffusion coefficient *D* of 4.8 x 10^{-10} m^2s^{-1} and 4.6 x 10^{-10} m^2s^{-1}, respectively (figure 29). According to the Stokes-Einstein equation these values correspond to objects with diameters of 2.2 and 2.3 nm. These values are in good agreement with the expected size of the dimeric capsules. Furthermore, ESI-MS measurements provided clear evidence of the formation of the [N···I⁺···N] halogen-bonded dimeric capsules **63a** and **63b**. The capsules were observed as $[\mathbf{57a}_2 \cdot I_4 \cdot OTs_2]^{2+}$ and $[\mathbf{57b}_2 \cdot I_4 \cdot OTs_2]^{2+}$ ions at *m/z* 1549 and *m/z* 1662, respectively.

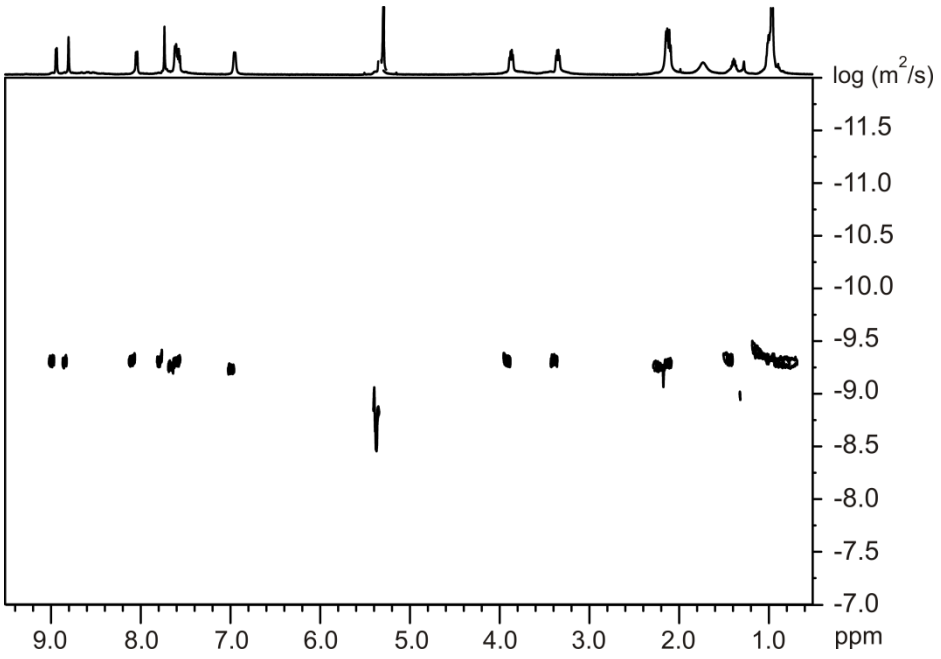

FIGURE 29 ^{1}H DOSY NMR spectrum of [N···I^{+}···N] halogen-bonded capsule **63a** (CD_2Cl_2, 400 MHz, 298 K).

Even though X-ray quality crystals were not obtained for [N···I^{+}···N] halogen-bonded dimeric capsules, the solution and gas-phase studies unambiguously supported the formation of the desired dimeric capsules. As results showed that [N···Ag^{+}···N] → [N···I^{+}···N] cation exchange can effectively be used in the construction of supramolecular capsules, it is likely that larger assemblies could be achieved by utilizing the same [N···Ag^{+}···N] → [N···I^{+}···N] cation exchange procedure with spatially complementary monomers.

2.5 Cavitand-based metal-ligand coordinated and [N···I^{+}···N] halogen-bonded hexameric capsules[III]

Based on the geometric features of the ethylene-bridged tetrakis(4-pyridyl)cavitand **58**, we speculated that utilizing multiple [N···I^{+}···N] halogen bonds an octahedral hexameric capsule could be obtained by applying the [N···Ag^{+}···N] → [N···I^{+}···N] cation exchange procedure (scheme 6).

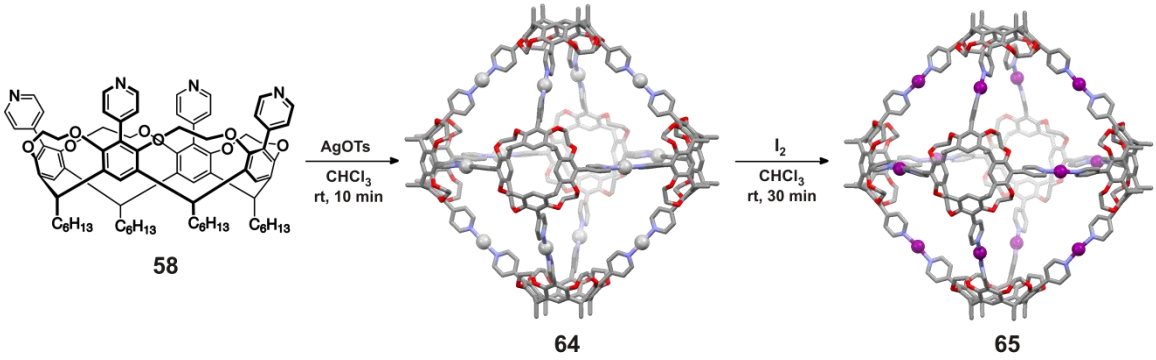

SCHEME 6 Synthesis of the [N···I⁺···N]-bridged hexameric capsule **65** through analogous Ag^+-coordination complex. For clarity, the hexyl side chains have been reduced to methyl groups and counterions are omitted.

The Ag^+-coordinated hexameric capsule **64** was synthesized by mixing ethylene-bridged tetrakis(4-pyridyl)cavitand **58** with AgOTs in a 1:2 ratio in $CDCl_3$. The ^1H NMR spectrum of **64** showed one set of signals with the expected complexation-induced shifts. ^1H DOSY NMR measurements further confirmed the formation of a single species with *D* of 2.2 x 10^{-10} m^2s^{-1} at 298 K in $CDCl_3$ (figure 30). Signals for smaller species were not observed. According to the Stokes-Einstein equation, the measured *D* corresponds to an object with diameter of 4.0 nm.

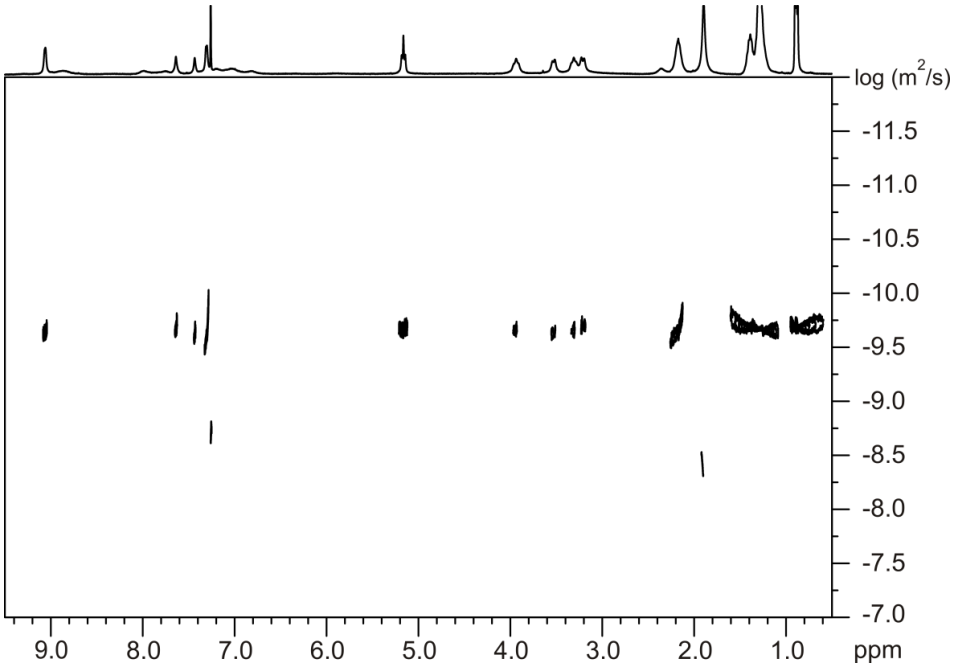

FIGURE 30 ^1H DOSY NMR spectrum of Ag^+-coordinated hexamer **64** ($CDCl_3$, 400 MHz, 298 K).

Furthermore, ESI-MS measurements supported the formation of the [N···Ag^+···N]-bridged hexamer **64** (figure 31). The gas-phase studies showed

mainly the desired metal-ligand coordinated hexamers in a charge state of 4+. The number of coordinated Ag^+-atoms varied from 8 to 12; the base peak was assigned to $[\mathbf{58}_6 \cdot Ag_9 \cdot OTs_5]^{4+}$ species at m/z 2313.

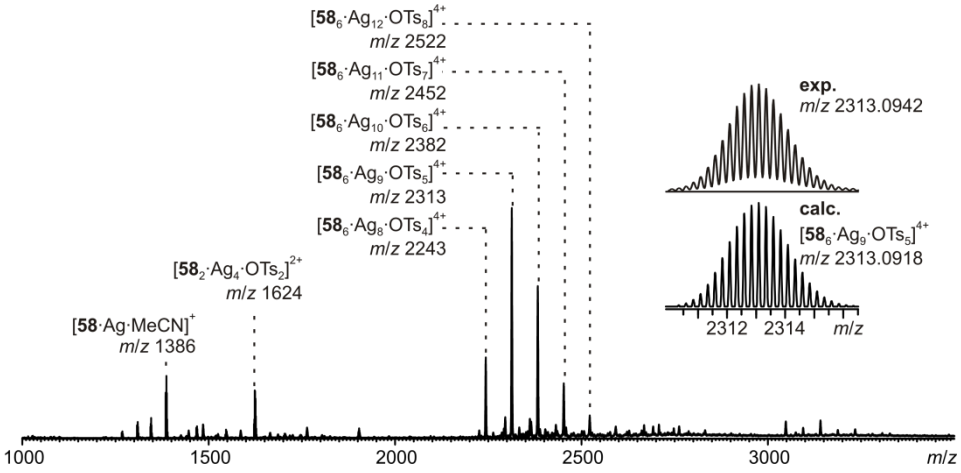

FIGURE 31 ESI-MS spectrum of [N···Ag^+···N]-bridged hexamer **64**.

Addition of molecular iodine into the $CDCl_3$ solution of Ag^+-hexamer **64** resulted in the formation of the [N···I^+···N] halogen-bonded assembly **65**. The ^1H NMR spectrum of **65** showed one set of well-resolved shifted signals indicating the formation of a discrete species. Selective formation of the [N···I^+···N]-bridged species was further confirmed by ^1H DOSY measurements. The ^1H DOSY spectrum showed single species with D of 2.3 x 10^{-10} m^2s^{-1} at 298 K in $CDCl_3$ (figure 32). Again, signals for smaller species were not observed. The calculated size corresponds to an object with diameter of 4.0 nm. The size is in a good agreement with the observed size of the Ag^+-coordinated hexamer **64**.

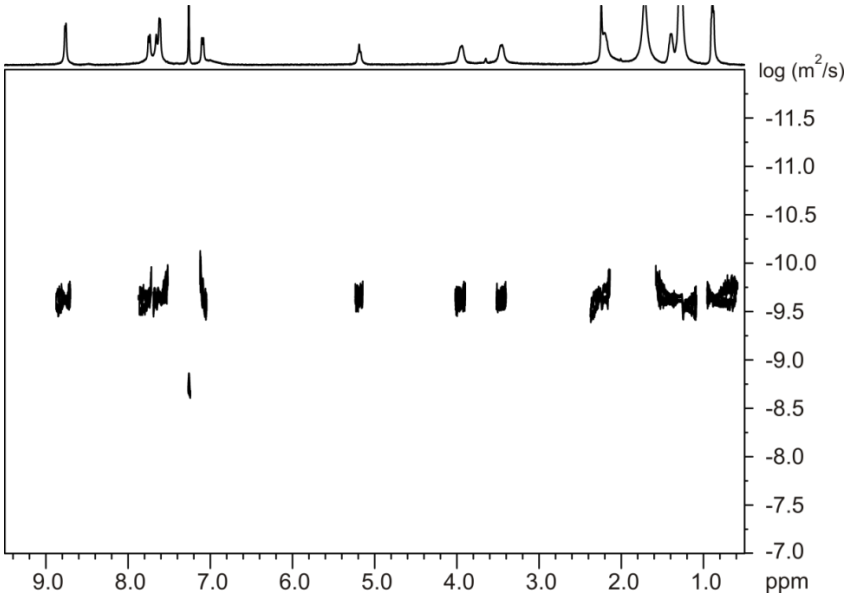

FIGURE 32 ^1H DOSY NMR spectrum of [N···I^+···N] halogen-bonded hexamer **65** ($CDCl_3$, 400 MHz, 298 K).

$^{1}H,^{15}N$ – heteronuclear multiple-bond correlation (HMBC) experiments have been used to study the formation of the [N···I^{+}···N] halogen bonds; the bond formation typically causes a shift of more than 100 ppm compared to the corresponding non-coordinated nitrogen.[121, 123,125] For the hexamer **65**, a single ^{15}N NMR signal at -176 ppm was observed. As the ^{15}N NMR signal for non-coordinated cavitand **58** was at -71 ppm, the formation of [N···I^{+}···N] halogen bonds was highly supported.

A 100 μM solution of hexamer **65** in $CHCl_3$/ACN 9:1 was prepared for the ESI-MS measurements. The spectrum showed the selective formation of I^{+}-hexamers in charge states 7+ to 5+ (figure 33). All observed high abundant complexes have a [**58**$_6$·I_{12}]$^{12+}$- core, the [**58**$_6$·I_{12}·OTs_6]$^{6+}$ species at *m*/*z* 1662 being the base peak.

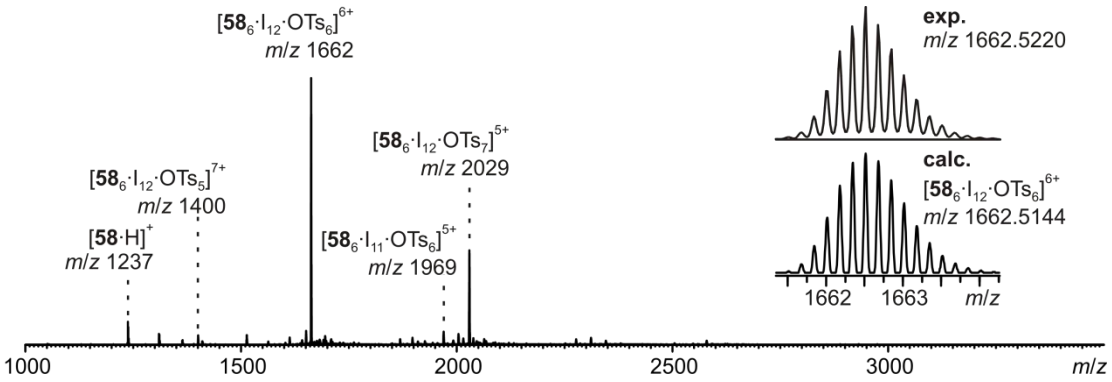

FIGURE 33 ESI-MS spectrum of [N···I^{+}···N] halogen-bonded hexamer **65**.

Unfortunately, crystallographic studies on hexameric capsules **64** and **65** could not be performed as suitable crystals were not obtained. However, this is not very surprising, as growing single crystals is not trivial for large molecular systems. Therefore, the structures of capsules **64** and **65** were modelled at the MM-level (SPARTAN16[148]). The modelling resulted in octahedral hexameric capsules **64** and **65** with a 4.3 - 4.5 nm diameter supporting the results obtained in solution and in the gas phase.

2.6 Metal-ligand coordinated and [N···I^{+}···N] halogen-bonded M_6L_4 and M_3L_2 cages from tripodal *N*-donor ligands[IV]

The applicability of multiple [N···I^{+}···N] halogen bonds in the formation of supramolecular assemblies was further investigated with tripodal ligands functionalized with two structurally different *N*-donor moieties (scheme 7). Both ligands, **60** and **61**, are known building blocks for coordination cages; therefore the formation of Ag^{+}-coordination cages **66** and **68** should be feasible (scheme 7). Furthermore, halogen-bonded cages **67** and **69** should be obtained

by applying the [N···Ag⁺···N] → [N···I⁺···N] cation exchange procedure (section 2.2.5).

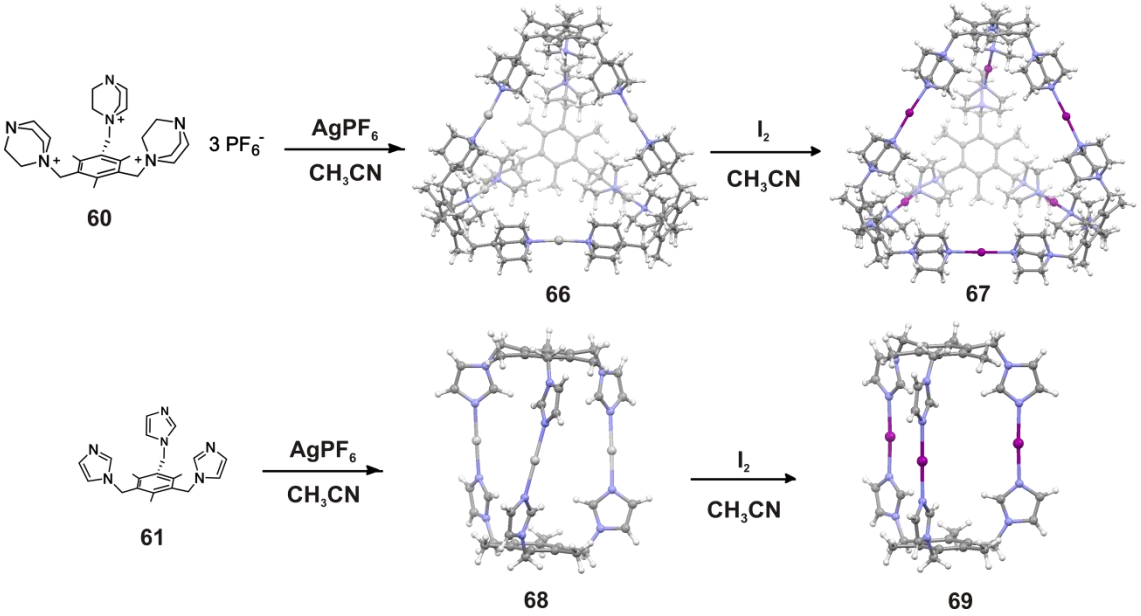

SCHEME 7 Syntheses of coordination cages **66** and **68** and [N···I⁺···N] halogen-bonded cages **67** and **69**. Counterions are omitted for clarity.

The self-assembly of **60** is highly affected by the intra- and intermolecular steric interactions of the bulky DABCO groups and the formation of tetrahedral M_6L_4 species is expected.[149] Generally used solvents such as DCM and $CHCl_3$ could not be used due to the poor solubility of the ligands and acetonitrile was chosen as the solvent. Even though acetonitrile is competing for the coordination to the I^+, as reported by Erdelyi and coworkers[123], the change of solvent was not expected to greatly hinder the formation of the [N···I⁺···N] halogen bonds.

The formation of cage **66** was investigated in solution by ^{1}H NMR. Surprisingly, the addition of $AgPF_6$ into the CD_3CN solution of ligand **60** did not result in noticeable shifts of the ligand proton signals in a ^{1}H NMR spectrum. Also, no evidence for the formation of **66** was found in ESI-MS measurements.

As neither ^{1}H NMR nor ESI-MS measurements supported the formation of cage **66**, crystallization of the desired tetramer was attempted. Unfortunately, suitable crystals were not obtained from the corresponding acetonitrile solution. However, crystals of the coordination cage **66** were obtained from a methanol solution of $AgPF_6$ and **60** upon slow diffusion with ethyl acetate (figure 34). The structure exhibits two-fold disorder of the tetrahedral cage framework, as has been previously observed with the corresponding Cu_6**60**$_4$ cage.[149]

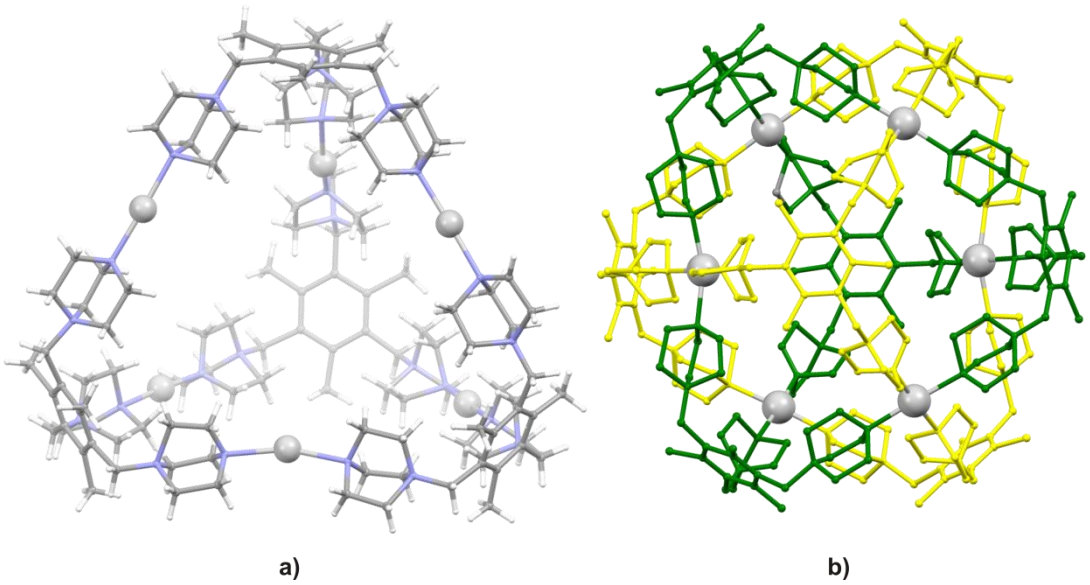

FIGURE 34 a) Crystal structure of **66** and b) disorder obtained in the crystal structure of **66**. Solvent molecules and counter anions are omitted for clarity.

Even though **60** did not form complexes with $AgPF_6$ in acetonitrile, addition of molecular iodine into a CD_3CN solution of **60** and $AgPF_6$ led to immediate precipitation of AgI and a color change of the initially colorless solution to yellow. The ^1H NMR spectrum showed a new set of downfield-shifted signals together with minor peaks of non-coordinated **60**. Also, ^1H DOSY measurements confirmed the formation of a new considerably larger assembly with D of 6.09 x 10^{-10} $m^2 \cdot s^{-1}$ in acetonitrile at 298 K. According to the Stokes –Einstein equation, the value of D corresponds to on object with diameter of 2.1 nm, which is in agreement with the size of the $M_6\mathbf{60}_4$ species.

Unfortunately, the investigation of **67** in the gas phase was unsuccessful. The stabilizing solvent and anion interaction are absent in the gas phase and due to the high charge density of **67** the complex was not stable enough to be analysed in gas phase.

Slow evaporation of the NMR sample of **67** over several weeks resulted in the formation of crystals suitable for X-ray diffraction. Crystal structure revealed the formation of the speculated tetrahedral [N···I^+···N] halogen-bonded cage **67** (figure 35). The N···I^+ bonds of **67** were slightly asymmetric with distances of 2.296 - 2.346 Å and the bond angles of [N···I^+···N] were close to linear, 175.3(1)°. The diameter of the **67** is roughly 2.1 nm according to the largest intramolecular H···H separation, which is in good agreement with the calculated size from the DOSY measurement.

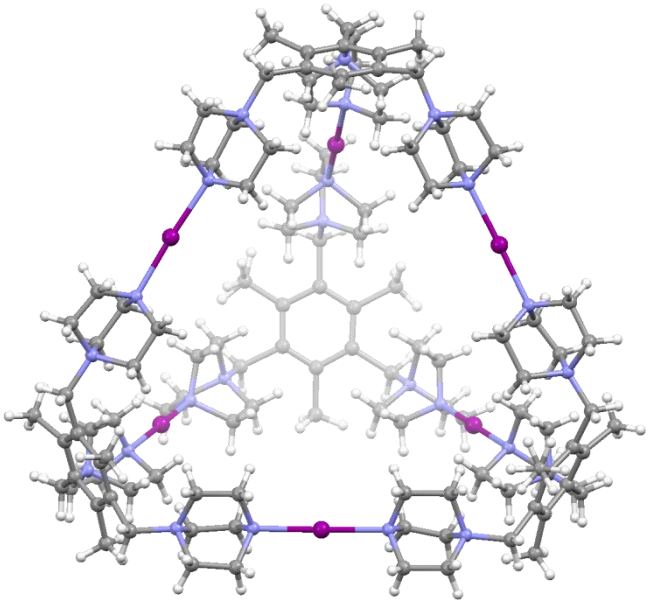

FIGURE 35 Crystal structure of **67**. Solvent molecules and counter anions are omitted for clarity.

Next, the focus was turned to imidazole-based ligand **61**. Even though neutral ligand **61** is capable of adapting different geometries due to the flexibility of the imidazole arms, selective formation of [N···I$^+$···N] halogen-bonded dimers was observed in solution and in solid state as well as in the gas phase.

^{1}H NMR spectra were measured for cages **68** and **69** and a new shifted set of signals was observed in both cases (figure 36). Furthermore, ^{1}H DOSY measurements of **68** and **69** in CD_3CN solutions confirmed the formation of single species with *D* of 8.46 x 10^{-10} $m^2 \cdot s^{-1}$ and 7.86 x 10^{-10} $m^2 \cdot s^{-1}$, respectively.

The composition of **69** was further studied in the gas phase by ESI-MS. The ESI-MS measurements confirmed the formation of M_3**61**$_2$ complexes, as ions [I_3**61**$_2$]$^{3+}$ at *m/z* 367 and [I_3**61**$_2$·PF_6]$^{2+}$ at *m/z* 623 were observed.

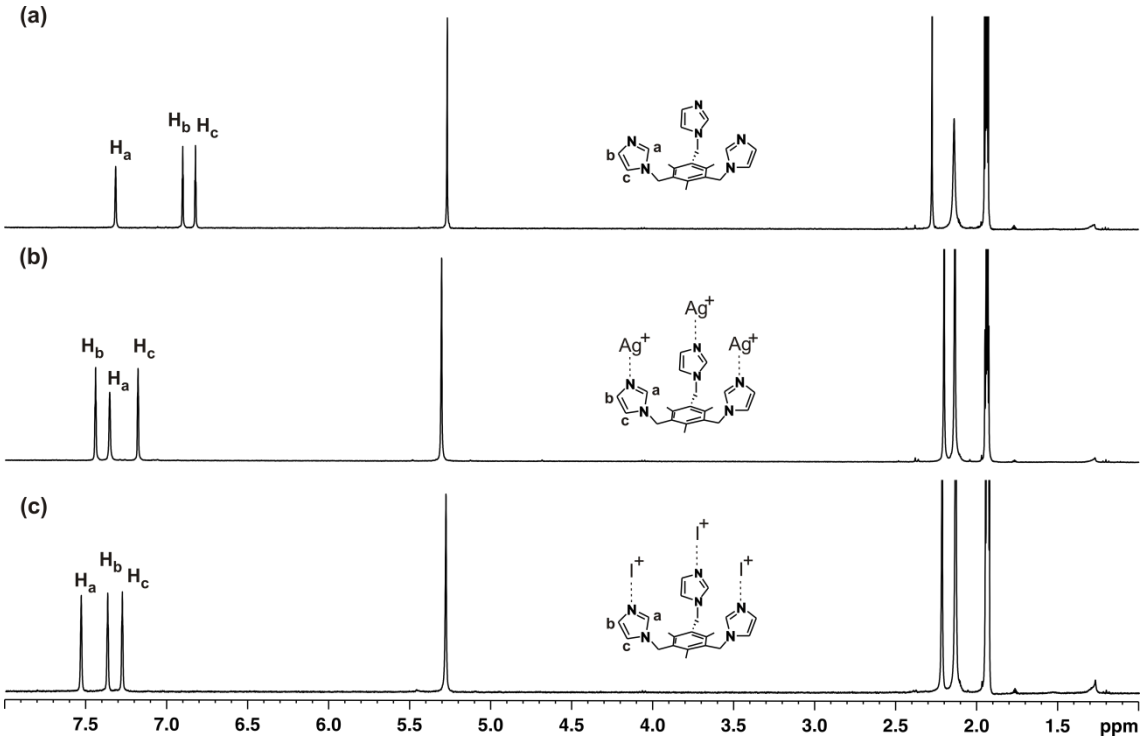

FIGURE 36 ^{1}H NMR spectra (CD_3CN, 400 MHz, 298 K) of a) **61**, b) **68** and c) **69**.

Finally, slow evaporation of an acetonitrile solution of iodonium complex of **61** resulted in the formation of single crystals of [N···I⁺···N] halogen-bonded "sandwich"-like M_3L_2 species (figure 36). The N···I⁺ bonds of **69** were symmetric with distances of 2.233(6) Å and the bond angles of [N···I⁺···N] XBs were close to linear, 176.9(4)°.

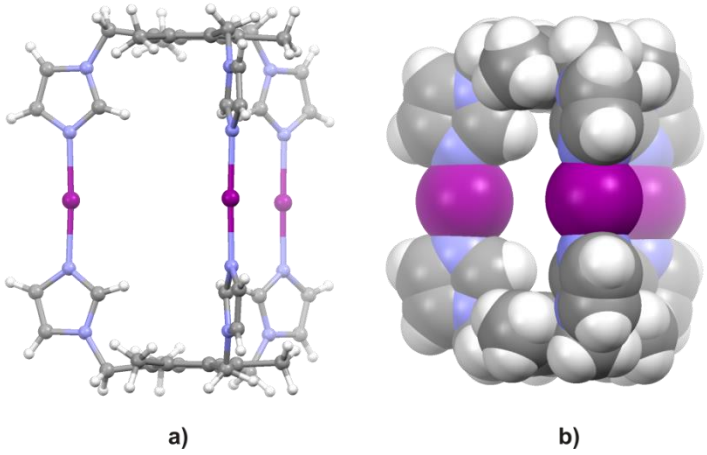

FIGURE 37 Crystal structure of **69** presented a) in ball-and-stick mode and b) in space-filling mode. Counteranions and solvent molecules are omitted for clarity.

3 CONCLUSIONS

In conclusion, this thesis describes the synthesis of multivalent halogen bond donors and acceptors based on resorcinarene cavitands and studies of their utilization in the formation of halogen-bonded architectures and assemblies. The use of tripodal *N*-donor ligands in [N···I$^+$···N] halogen-bonded complexes was also investigated.

The attachment of four iodo- or bromoacetylene groups to methylene-bridged cavitands resulted in the formation of rigid and symmetric multivalent XB donor molecules. Crystallization of **54** from 1,4-dioxane resulted in the formation of a halogen-bonded complex where **54** behaved as a trivalent XB donor. Due to strong C-H···C≡C interactions, cavitand **54** showed strong self-inclusion behaviour, which resulted in the formation of a dimeric structure with one of the iodoethynyl groups complexed into the cavity of the second cavitand.

To prevent the formation of the self-inclusion dimer, more flexible ethylene-bridged cavitands were used. The strategy was successful, as the formation of the self-inclusion dimer was not observed in the subsequent solid-state assemblies. Cavitand **56** was then used as a tetravalent XB donor leading to halogen-bonded architectures with mono- and divalent halogen bond acceptor moieties.

The [N···Ag$^+$···N] → [N···I$^+$···N] cation exchange reaction was utilized in the construction of halogen-bonded capsules and cages. The 3*c*4*e* [N···I$^+$···N] bond is highly directional and enabled, by carefully designed preorganized monomers, the synthesis of several supramolecular assemblies.

In order to exploit multiple [pyridine···I$^+$···pyridine] interactions as structural units in the capsules, ethylene-bridged tetrakis(pyridyl)cavitands **57** and **58** were chosen as building blocks. Cavitands **57** and **58** are rigid enough, but at the same time also flexible enough, to tolerate small changes from the optimal geometry that might be required for the formation of multiple linear [N···Ag$^+$···N] coordination bonds or [N···I$^+$···N] XBs.

NMR studies of dimeric Ag$^+$-capsules **62a** and **62b** revealed a formation of mixture of species, which was also supported by the crystal structure of **62a** as two structurally different centrosymmetric dimeric capsules.

^{1}H NMR spectra of capsules **63a** and **63b** showed selective formation of symmetrical [N···I$^+$···N] halogen-bonded capsules. ^{1}H DOSY and ESI-MS measurements further provided clear evidence of the formation of [N···I$^+$···N] halogen-bonded dimeric capsules **63a** and **63b**.

By changing the position of the pyridine N-atoms from *meta* to *para*, ethylene-bridged tetrakis(pyridyl)cavitands were used to form octahedral hexameric capsules. Intermediate hexameric Ag$^+$-capsule **64** was obtained in solution and in the gas phase. Subsequent cation exchange selectively provided the hexameric [N···I$^+$···N] halogen-bonded capsule **65**, which was characterized in solution as well as in the gas phase.

The general applicability of the [N···Ag$^+$···N] → [N···I$^+$···N] cation exchange procedure to form halogen-bonded supramolecular assemblies was further studied with two different tripodal *N*-donor ligands **60** and **61**. As both ligands are known building blocks for coordination cages, the [N···I$^+$···N] XBs was expected to yield halonium cages **67** and **69**.

Even though no evidence of the formation of the metal-ligand coordinated cage **66** in acetonitrile was obtained in solution or in the gas phase, **67** could be synthesized by adding iodine to the acetonitrile solution of **60** and $AgPF_6$. Cage **67** was also crystallized by slowly evaporating the corresponding acetonitrile solution. Selective formation of cages **68** and **69** was confirmed in solution, in the gas phase as well as in the solid state.

In conclusion, the results presented here show that halogen bonding can be used as a predictable tool in the construction of well-defined supramolecular assemblies from preorganized multivalent monomers. The use of halogen(I) ions as connecting elements in the self-assembly processes of large supramolecular assemblies is a rather unexplored area, but it should not be overlooked. There is still much to be discovered in the utilization of the [N···Ag$^+$···N] → [N···I$^+$···N] cation exchange reaction and generally in halogen bonding.

REFERENCES

1. P. Politzer, J. S. Murray, T. Clark, *Phys. Chem. Chem. Phys.* **2013**, *15*, 11178–11189.
2. F. Guthrie, *J. Chem. Soc.* **1863**, *16*, 239–244.
3. R. S. Mulliken, *J. Am. Chem. Soc.* **1950**, *72*, 600–608.
4. O. Hassel, *Science* **1970**, *170*, 497–502.
5. O. Hassel, J. Hvoslef, *Acta Chem. Scand.* **1954**, *8*, 873.
6. E. Gunnar, O. Hassel, *Acta Chem. Scand.* **1956**, *10*, 139–141.
7. O. Hassel, K. O. Stromme, *Acta Chem. Scand.* **1958**, *12*, 1146.
8. O. Hassel, K. O. Stromme, *Nature* **1958**, *182*, 1155–1156.
9. T. Bjorvatten, O. Hassel, *Acta Chem. Scand.* **1961**, *15*, 1429–1436.
10. N. Ramasubbu, R. Parthasarathy, P. Murray-Rust, *J. Am. Chem. Soc.* **1986**, *108*, 4308–4314.
11. J. P. M. Lommerse, A. J. Stone, R. Taylor, F. H. Allen, *J. Am. Chem. Soc.* **1996**, *118*, 3108–3116.
12. A. C. Legon, *Chem. Eur. J.* **1998**, *4*, 1890–1897.
13. A. C. Legon, *Angew. Chem. Int. Ed.* **1999**, *38*, 2686–2714.
14. V. Amico, S. V. Meille, E. Corradi, M. T. Messina, G. Resnati, *J. Am. Chem. Soc.* **1998**, *120*, 8261–8262.
15. E. Corradi, S. V. Meille, M. T. Messina, P. Metrangolo, G. Resnati, *Angew. Chem. Int. Ed.* **2000**, *39*, 1782–1786.
16. P. Metrangolo, G. Resnati, *Chem. Eur. J.* **2001**, *7*, 2511–2519.
17. R. A. Zingaro, R. M. Hedges, *J. Phys. Chem.* **1961**, *65*, 1132–1138.
18. D. E. Martire, J. P. Sheridan, J. W. King, S. E. O'Donnell, *J. Am. Chem. Soc.* **1976**, *98*, 3101–3106.
19. J.-M. Dumas, H. Peurichard, M. J. Gomel, *J. Chem. Res.* **1978**, *2*, 54.
20. S. C. Blackstock, J. P. Lorand, J. K. Kochi, *J. Org. Chem.* **1987**, *52*, 1451–1460.
21. G. R. Desiraju, P. S. Ho, L. Kloo, A. C. Legon, R. Marquardt, P. Metrangolo, P. Politzer, G. Resnati, K. Rissanen, *Pure Appl. Chem.* **2013**, *85*, 1711–1713.
22. T. Clark, M. Hennemann, J. S. Murray, P. Politzer, *J. Mol. Model.* **2007**, *13*, 291–296.
23. P. Politzer, J. S. Murray, T. Clark, *Phys. Chem. Chem. Phys.* **2010**, *12*, 7748–7757.
24. S. M. Huber, E. Jimenez-Izal, J. M. Ugalde, I. Infante, *Chem. Commun.* **2012**, *48*, 7708–7710.
25. S. M. Huber, J. D. Scanlon, E. Jimenez-Izal, J. M. Ugalde, I. Infante, *Phys. Chem. Chem. Phys.* **2013**, *15*, 10350–10357.
26. L. P. Wolters, F. M. Bickelhaupt, *ChemistryOpen* **2012**, *1*, 96–105.
27. C. C. Robertson, R. N. Perutz, L. Brammer, C. A. Hunter, *Chem. Sci.* **2014**, *5*, 4179–4183.

28. P. Metrangolo, J. S. Murray, T. Pilati, P. Politzer, G. Resnati, G. Terraneo, *Cryst. Growth Des.* **2011**, *11*, 4238–4246.
29. P. Metrangolo, J. S. Murray, T. Pilati, P. Politzer, G. Resnati, G. Terraneo, *CrystEngComm* **2011**, *13*, 6593–6596.
30. P. Metrangolo, H. Neukirch, T. Pilati, G. Resnati, *Acc. Chem. Res.* **2005**, *38*, 386–395.
31. C. Präsang, A. C. Whitwood, D. W. Bruce, *Cryst. Growth Des.* **2009**, *9*, 5319–5326.
32. P. Metrangolo, T. Pilati, G. Terraneo, S. Biella, G. Resnati, *CrystEngComm* **2009**, *11*, 1187–1196.
33. D. Cinčić, T. Friščić, W. Jones, *Chem. Eur. J.* **2008**, *14*, 747–753.
34. J. I. Jay, C. W. Padgett, R. D. B. Walsh, T. W. Hanks, W. T. Pennington, *Cryst. Growth Des.* **2001**, *1*, 501–507.
35. L. Brammer, E. A. Bruton, P. Sherwood, *Cryst. Growth Des.* **2001**, *1*, 277–290.
36. F. Zordan, L. Brammer, P. Sherwood, *J. Am. Chem. Soc.* **2005**, *127*, 5979–5989.
37. P. Cardillo, E. Corradi, A. Lunghi, V. Meille, M. T. Messina, P. Metrangolo, G. Resnati, *Tetrahedron* **2000**, *56*, 5535–5550.
38. R. B. Walsh, C. W. Padgett, P. Metrangolo, G. Resnati, T. W. Hanks, W. T. Pennington, *Cryst. Growth Des.* **2001**, *1*, 165–175.
39. D. D. Burton, F. Fontana, P. Metrangolo, T. Pilati, G. Resnati, *Tetrahedron Lett.* **2003**, *44*, 645–648.
40. R. Liantonio, P. Metrangolo, T. Pilati, G. Resnati, A. Stevenazzi, *Cryst. Growth Des.* **2003**, *3*, 799–803.
41. P. Metrangolo, T. Pilati, G. Resnati, A. Stevenazzi, L. Via, *Chem. Commun.* **2004**, 1492–1493.
42. Q. Chu, Z. Wang, Q. Huang, C. Yan, S. Zhu, *J. Am. Chem. Soc.* **2001**, *123*, 11069–11070.
43. R. Liantonio, P. Metrangolo, F. Meyer, T. Pilati, W. Navarrini, G. Resnati, *Chem. Commun.* **2006**, 1819–1821.
44. P. Metrangolo, Y. Carcenac, M. Lahtinen, T. Pilati, K. Rissanen, A. Vij, G. Resnati, *Science* **2009**, *323*, 1461–1464.
45. H. M. Yamamoto, R. Kato, *Chem. Lett.* **2000**, *29*, 970–971.
46. A. De Santis, A. Forni, R. Liantonio, P. Metrangolo, T. Pilati, G. Resnati, *Chem. Eur. J.* **2003**, *9*, 3974–3983.
47. D. Cinčić, T. Friščić, W. Jones, *J. Am. Chem. Soc.* **2008**, *130*, 7524–7525.
48. P. Cauliez, V. Polo, T. Roisnel, R. Llusar, M. Fourmigué, *CrystEngComm* **2010**, *12*, 558–566.
49. C. B. Lucassen, A. Karton, G. Leitus, L. J. W. Shimon, J. M. L. Martin, M. E. Van Der Boom, *Cryst. Growth Des.* **2007**, *7*, 386–392.
50. P. Metrangolo, F. Meyer, P. Tullio, G. Resnati, G. Terraneo, *Chem. Commun.* **2008**, 1635–1637.
51. P. Metrangolo, F. Meyer, T. Pilati, D. M. Proserpio, G. Resnati, *Chem. Eur. J.* **2007**, *13*, 5765–5772.

52. R. Thaimattam, C. V. K. Sharma, A. Clearfield, G. R. Desiraju, *Cryst. Growth Des.* **2001**, *1*, 103–106.
53. P. Metrangolo, W. Panzeri, F. Recupero, G. Resnati, *J. Fluor. Chem.* **2002**, *114*, 27–33.
54. A. Mele, P. Metrangolo, H. Neukirch, T. Pilati, G. Resnati, *J. Am. Chem. Soc.* **2005**, *127*, 14972–14973.
55. M. G. Sarwar, B. Dragisic, S. Sagoo, M. S. Taylor, *Angew. Chem. Int. Ed.* **2010**, *49*, 1674–1677.
56. E. Dimitrijević, O. Kvak, M. S. Taylor, *Chem. Commun.* **2010**, *46*, 9025–9027.
57. M. G. Sarwar, B. Dragisić, E. Dimitrijević, M. S. Taylor, *Chem. Eur. J.* **2013**, *19*, 2050–2058.
58. F. Kniep, S. H. Jungbauer, Q. Zhang, S. M. Walter, S. Schindler, I. Schnapperelle, E. Herdtweck, S. M. Huber, *Angew. Chem. Int. Ed.* **2013**, *52*, 7028–7032.
59. S. H. Jungbauer, D. Bulfield, F. Kniep, C. W. Lehmann, E. Herdtweck, S. M. Huber, *J. Am. Chem. Soc.* **2014**, *136*, 16740–16743.
60. S. H. Jungbauer, S. Schindler, E. Herdtweck, S. Keller, S. M. Huber, *Chem. Eur. J.* **2015**, *21*, 13625–13636.
61. H. L. Nguyen, P. N. Horton, M. B. Hursthouse, A. C. Legon, D. W. Bruce, *J. Am. Chem. Soc.* **2004**, *126*, 16–17.
62. P. Metrangolo, C. Präsang, G. Resnati, R. Liantonio, A. C. Whitwood, D. W. Bruce, *Chem. Commun.* **2006**, *323*, 3290–3292.
63. J. Xu, X. Liu, T. Lin, J. Huang, C. He, *Macromolecules* **2005**, *38*, 3554–3557.
64. R. Bertani, P. Metrangolo, A. Moiana, E. Perez, T. Pilati, G. Resnati, I. Rico-Lattes, A. Sassi, *Adv. Mater.* **2002**, *14*, 1197–1201.
65. N. Houbenov, R. Milani, M. Poutanen, J. Haataja, V. Dichiarante, J. Sainio, J. Ruokolainen, G. Resnati, P. Metrangolo, O. Ikkala, *Nat. Commun.* **2014**, *5*, 1–8.
66. L. Meazza, J. A. Foster, K. Fucke, P. Metrangolo, G. Resnati, J. W. Steed, *Nat. Chem.* **2013**, *5*, 42–47.
67. W. Dehn, *J. Am. Chem. Soc.* **1911**, *33*, 1598–1601.
68. B. Borgen, O. Hassel, C. Römming, *Acta Chem. Scand.* **1962**, *16*, 2469–2470.
69. T. Bjorvatten, *Acta Chem. Scand.* **1968**, *22*, 410–420.
70. M. Ghassemzadeh, K. Harms, K. Dehnicke, *Chem. Ber.* **1996**, *129*, 259–262.
71. C. Perkins, S. Libri, H. Adams, L. Brammer, *CrystEngComm* **2012**, *14*, 3033–3038.
72. C. B. Aakeröy, T. K. Wijethunga, J. Desper, M. Đaković, *Cryst. Growth Des.* **2015**, *15*, 3853–3861.
73. O. Dumele, D. Wu, N. Trapp, N. Goroff, F. Diederich, *Org. Lett.* **2014**, *16*, 4722–4725.
74. C. B. Aakeröy, M. Baldrighi, J. Desper, P. Metrangolo, G. Resnati, *Chem. Eur. J.* **2013**, *19*, 16240–16247.
75. N. S. Goroff, S. M. Curtis, J. A. Webb, F. W. Fowler, J. W. Lauher, *Org. Lett.* **2005**, *7*, 1891–1893.
76. A. Sun, J. W. Lauher, N. S. Goroff, *Science* **2006**, *312*, 1030–1034.

77. H. M. Yamamoto, J. I. Yamaura, R. Kato, *J. Am. Chem. Soc.* **1998**, *120*, 5905–5913.
78. H. M. Yamamoto, J. I. Yamaura, R. Kato, *Synth. Met.* **1999**, *102*, 1448–1451.
79. H. M. Yamamoto, R. Maeda, J.-I. Yamaura, R. Kato, *J. Mater. Chem.* **2001**, *11*, 1034–1041.
80. H. M. Yamamoto, Y. Kosaka, R. Maeda, J. I. Yamaura, A. Nakao, T. Nakamura, R. Kato, *ACS Nano* **2008**, *2*, 143–155.
81. J. Lieffrig, H. M. Yamamoto, T. Kusamoto, H. Cui, O. Jeannin, M. Fourmigué, R. Kato, *Cryst. Growth Des.* **2011**, *11*, 4267–4271.
82. J. Lieffrig, O. Jeannin, M. Fourmigue, *J. Am. Chem. Soc.* **2013**, *135*, 6200–6210.
83. M. Ghassemzadeh, K. Harms, K. Dehnicke, J. Magull, *Z. Naturforsch., B J. Chem. Sci.* **1994**, *49*, 506–512.
84. M. Ghassemzadeh, K. Harms, K. Dehnicke, D. Fenske, *Z. Naturforsch., B J. Chem. Sci.* **1994**, *49*, 593–601.
85. M. Ghassemzadeh, K. Dehnicke, H. Goesmann, D. Fenske, *Z. Naturforsch., B J. Chem. Sci.* **1994**, *49*, 602–608.
86. E. H. Crowston, A. M. Lobo, S. Prabhakar, H. S. Rzepa, D. J. Williams, *J. Chem. Soc., Chem. Commun.* **1984**, 276–278.
87. K. Raatikainen, K. Rissanen, *CrystEngComm* **2011**, *13*, 6972–6977.
88. K. Raatikainen, K. Rissanen, *Chem. Sci.* **2012**, *3*, 1235.
89. D. Dolenc, B. Modec, *New J. Chem.* **2009**, *33*, 2344–2349.
90. O. Makhotkina, J. Lieffrig, O. Jeannin, M. Fourmigué, E. Aubert, E. Espinosa, *Cryst. Growth Des.* **2015**, *15*, 3464–3473.
91. R. Puttreddy, O. Jurček, S. Bhowmik, T. Mäkelä, K. Rissanen, *Chem. Commun.* **2016**, *52*, 2338–2341.
92. I. Nicolas, F. Barriere, O. Jeannin, M. Fourmigué, *Cryst. Growth Des.* **2016**, *16*, 2963–2971.
93. A. Caballero, N. G. White, P. D. Beer, *Angew. Chem. Int. Ed.* **2011**, *50*, 1845–1848.
94. F. Zapata, A. Caballero, N. G. White, T. D. W. Claridge, P. J. Costa, V. Félix, P. D. Beer, *J. Am. Chem. Soc.* **2012**, *134*, 11533–11541.
95. R. Tepper, B. Schulze, M. Jäger, C. Friebe, D. H. Scharf, H. Görls, U. S. Schubert, *J. Org. Chem.* **2015**, *80*, 3139–3150.
96. R. Tepper, B. Schulze, H. Görls, P. Bellstedt, M. Jäger, U. S. Schubert, *Org. Lett.* **2015**, *17*, 5740–5743.
97. C. J. Serpell, N. L. Kilah, P. J. Costa, V. Félix, P. D. Beer, *Angew. Chem. Int. Ed.* **2010**, *49*, 5322–5326.
98. N. L. Kilah, M. D. Wise, C. J. Serpell, A. L. Thompson, N. G. White, K. E. Christensen, P. D. Beer, *J. Am. Chem. Soc.* **2010**, *132*, 11893–11895.
99. A. Caballero, S. Bennett, C. J. Serpell, P. D. Beer, *CrystEngComm* **2013**, *15*, 3076–3081.
100. M. J. Langton, S. W. Robinson, I. Marques, V. Félix, P. D. Beer, *Nat. Chem.* **2014**, *6*, 1039–1043.
101. J. L. Atwood, L. R. MacGillivray, *Nature* **1997**, *389*, 469–472.

102. T. Heinz, D. M. Rudkevich, J. Rebek Jr., *Nature* **1998**, *394*, 764–766.
103. C. B. Aakeröy, A. Rajbanshi, P. Metrangolo, G. Resnati, M. F. Parisi, J. Desper, T. Pilati, *CrystEngComm* **2012**, *14*, 6366–6368.
104. N. K. Beyeh, F. Pan, K. Rissanen, *Angew. Chem. Int. Ed.* **2015**, *54*, 7303–7307.
105. F. Pan, N. K. Beyeh, K. Rissanen, *J. Am. Chem. Soc.* **2015**, *137*, 10406–10413.
106. O. Dumele, N. Trapp, F. Diederich, *Angew. Chem. Int. Ed.* **2015**, *54*, 12339–12344.
107. O. Dumele, B. Schreib, U. Warzok, N. Trapp, C. A. Schalley, F. Diederich, *Angew. Chem. Int. Ed.* **2017**, 1152–1157.
108. L. Koskinen, P. Hirva, E. Kalenius, S. Jääskeläinen, K. Rissanen, M. Haukka, *CrystEngComm* **2015**, *17*, 1231–1236.
109. O. Hassel, H. Hope, *Acta Chem. Scand.* **1961**, *15*, 407–416.
110. H. Pritzkow, *Acta Cryst.* **1975**, *20*, 1505–1506.
111. N. W. Alcock, G. B. Robertson, *J. Chem. Soc., Dalton Trans.* **1975**, 2483–2486.
112. B. Y. G. D. Brayer, M. N. G. James, C. Tg, *Acta Cryst.* **1982**, *B38*, 654–657.
113. L. K. Blair, K. D. Parris, P. Sen Hii, C. P. Brock, H. Acta, *J. Am. Chem. Soc.* **1983**, *105*, 3649–3653.
114. C. Pratt Brock, Y. Fu, *Acta Cryst.* **1988**, *30*, 1582–1585.
115. A. A. Neverov, R. S. Brown, *J. Org. Chem.* **1998**, *63*, 5977–5982.
116. A. A. Neverov, H. X. Feng, K. Hamilton, R. S. Brown, *J. Org. Chem.* **2003**, *68*, 3802–3810.
117. B. Y. G. D. Brayer, M. N. G. James, C. Tg, **1982**, 654–657.
118. M. J. Crawford, M. Göbel, K. Karaghiosoff, T. M. Klapötke, J. M. Welch, *Inorg. Chem.* **2009**, *48*, 9983–9985.
119. J. Barluenga, *Pure Appl. Chem.* **1999**, *71*, 431–436.
120. C. Álvarez-Rúa, S. García-Granda, A. Ballesteros, F. González-Bobes, J. M. González, *Acta Cryst.* **2002**, *E58*, o1381–o1383.
121. A. C. C. Carlsson, J. Gräfenstein, A. Budnjo, J. L. Laurila, J. Bergquist, A. Karim, R. Kleinmaier, U. Brath, M. Erdelyi, *J. Am. Chem. Soc.* **2012**, *134*, 5706–5715.
122. A.-C. C. Carlsson, J. Gräfenstein, J. L. Laurila, J. Bergquist, M. Erdélyi, *Chem. Commun.* **2012**, *48*, 1458–60.
123. A.-C. C. Carlsson, M. Uhrbom, A. Karim, U. Brath, J. Gräfenstein, M. Erdélyi, *CrystEngComm* **2013**, *15*, 3087–3092.
124. A. Karim, M. Reitti, A.-C. C. Carlsson, J. Gräfenstein, M. Erdélyi, *Chem. Sci.* **2014**, *5*, 3226–3233.
125. M. Bedin, A. Karim, M. Reitti, A.-C. C. Carlsson, F. Topić, M. Cetina, F. Pan, V. Havel, F. Al-Ameri, V. Sindelar, K. Rissanen, J. Gräfenstein, M. Erdélyi, *Chem. Sci.* **2015**, *6*, 3746–3756.
126. A. C. C. Carlsson, K. Mehmeti, M. Uhrbom, A. Karim, M. Bedin, R. Puttreddy, R. Kleinmaier, A. A. Neverov, B. Nekoueishahraki, J. Gräfenstein, K. Rissanen, M. Erdélyi, *J. Am. Chem. Soc.* **2016**, *138*, 9853–9863.
127. S. B. Hakkert, M. Erdélyi, *J. Phys. Org. Chem.* **2015**, *28*, 226–233.
128. G. H.-Y. Lin, H. Hope, *Acta Cryst.* **1972**, *B28*, 643–646.

129. P. D. Boyle, J. Christie, T. Dyer, S. M. Godfrey, I. R. Howson, C. McArthur, B. Omar, R. G. Pritchard, G. R. Williams, *J. Chem. Soc., Dalton Trans.* **2000**, 3106–3112.
130. V. Daga, S. K. Hadjikakou, N. Hadjiliadis, M. Kubicki, J. H. Z. dos Santos, I. S. Butler, *Eur. J. Inorg. Chem.* **2002**, *2002*, 1718–1728.
131. G. J. Corban, S. K. Hadjikakou, N. Hadjiliadis, M. Kubicki, E. R. T. Tiekink, I. S. Butler, E. Drougas, A. M. Kosmas, *Inorg. Chem.* **2005**, *44*, 8617–8627.
132. A. Tamilselvi, G. Mugesh, *Bioorganic Med. Chem. Lett.* **2010**, *20*, 3692–3697.
133. M. S. Chernov'Yants, I. V. Burykin, Z. A. Starikova, N. E. Erofeev, *J. Mol. Struct.* **2011**, *1006*, 379–382.
134. F. Demartin, P. Deplano, F. A. Devillanova, F. Isaia, V. Lippois, G. Veranilb, *Inorg. Chem.* **1993**, *2*, 3694–3699.
135. E. Seppälä, F. Ruthe, J. Jeske, W. Mont, P. G. Jones, A. Chemie, T. U. Braunschweig, G. E-mail, *Chem. Commun.* **1999**, *1*, 1471–1472.
136. W. W. Du Mont, M. Bätcher, C. Daniliuc, F. A. Devillanova, C. Druckenbrodt, J. Jeske, P. G. Jones, V. Lippolis, F. Ruthe, E. Seppälä, *Eur. J. Inorg. Chem.* **2008**, 4562–4577.
137. S. T. Manjare, H. B. Singh, R. J. Butcher, *Eur. J. Inorg. Chem.* **2013**, 2161–2166.
138. L. Abis, E. Dalcanale, A. Du vosel, S. Sperala, *J. Org. Chem.* **1988**, *53*, 5475–5475.
139. L. M. Tunstad, J. A. Tucker, E. Dalcanale, J. Weiser, J. A. Bryant, J. C. Sherman, R. C. Helgeson, C. B. Knobler, D. J. Cram, *J. Org. Chem.* **1989**, *54*, 1305–1312.
140. J. A. Bryant, M. T. Blanda, M. Vincenti, D. J. Cram, *J. Am. Chem. Soc.* **1991**, *113*, 2167–2172.
141. F. Gruppi, F. Boccini, L. Elviri, E. Dalcanale, *Tetrahedron* **2009**, *65*, 7289–7295.
142. C. Grave, D. Lentz, A. Schäfer, J. P. Rabe, P. Franke, A. D. Schlüter, *J. Am. Chem. Soc.* **2003**, *125*, 6907–6918.
143. C. B. Aakeröy, N. Schultheiss, J. Desper, *CrystEngComm* **2007**, *9*, 211–214.
144. K. Osowska, T. Lis, S. Szafert, *Eur. J. Org. Chem.* **2008**, 4598–4606.
145. C. B. Aakeröy, P. D. Chopade, C. F. Quinn, J. Desper, *CrystEngComm* **2014**, *16*, 3796–3801.
146. P. J. Garratt, A. J. Ibbett, J. E. Ladbury, R. O'Brien, M. B. Hursthouse, K. M. A. Malik, *Tetrahedron* **1998**, *54*, 949–968.
147. Y. Yuan, Z. Jiang, J. Yan, G. Gao, A. S. C. Chan, R.-G. Xie, *Synth. Commun.* **2000**, *30*, 4555–4561.
148. Spartan'16, Wavefunct. Inc., Irvine, USA, **2016**.
149. A. Peuronen, S. Forsblom, M. Lahtinen, *Chem. Commun.* **2014**, *50*, 5469–5472.